Copy
RM L57J08

NACA RM L57J08

NACA

RESEARCH MEMORANDUM

INVESTIGATION AT HIGH SUBSONIC SPEEDS OF THE STATIC LONGITUDINAL AND LATERAL STABILITY CHARACTERISTICS OF TWO CANARD AIRPLANE CONFIGURATIONS

By William C. Sleeman, Jr.

Langley Aeronautical Laboratory
Langley Field, Va.

NATIONAL ADVISORY COMMITTEE
FOR AERONAUTICS

WASHINGTON

December 3, 1957

NATIONAL ADVISORY COMMITTEE FOR AERONAUTICS

RESEARCH MEMORANDUM

INVESTIGATION AT HIGH SUBSONIC SPEEDS OF THE STATIC LONGITUDINAL AND LATERAL STABILITY CHARACTERISTICS OF TWO CANARD AIRPLANE CONFIGURATIONS

By William C. Sleeman, Jr.

SUMMARY

The present investigation was conducted in the Langley high-speed 7- by 10-foot tunnel to determine the static longitudinal and lateral stability characteristics at high subsonic speeds of two canard airplane configurations previously tested at supersonic speeds. The Mach number range of this investigation extended from 0.60 to 0.94 and a maximum angle-of-attack range of -2° to 24° was obtained at the lowest test Mach number. Two wing plan forms of equal area were studied in the present tests; one was a 60° delta wing and the other was a trapezoid wing having an aspect ratio of 3, taper ratio of 0.143, and an unswept 80-percent-chord line. The canard control had a trapezoidal plan form and its area was approximately 11.5 percent of the wing area. The model also had a low-aspect-ratio highly swept vertical tail and twin ventral fins.

The longitudinal control characteristics of the models were consistent with past experience at low speed on canard configurations in that stalling of the canard surface occurred at moderate and high control deflections for moderate values of angle of attack. This stalling could impose appreciable limitations on the maximum trim-lift coefficient attainable. The control effectiveness and maximum value of trim lift was significantly increased by addition of a body flap having a conical shape and located slightly behind the canard surface on the bottom of the body.

Addition of the canard surface at 0° deflection had relatively little effect on overall directional stability of the delta-wing configuration; however, deflection of the canard surface from 0° to 10° had a large favorable effect on directional stability at high angles of attack for both the trapezoid- and delta-wing configurations.

INTRODUCTION

Present interest in canard airplane configurations arises from potential performance benefits possible at supersonic speeds in comparison to conventional tail-rearward and tailless airplane designs. The canard arrangement also offers a solution to problems of balance which are becoming more acute with the design trend toward more rearward engine placement and accompanying rearward center-of-gravity position, particularly for multiengine arrangements. The main problem encountered in the past for canard configurations was associated with stalling of the canard surface which severely limited the allowable center-of-gravity travel and the maximum trim lift of the airplane. (See ref. 1.) This problem as well as the directional stability difficulties found for some canard configurations indicated the existence of some formidable subsonic problems, and the potential rewards to be gained at subsonic speeds by using canard controls did not merit solution of these problems. The aforementioned supersonic performance benefits offer an effective stimulus to renewed effort on finding solutions for the known low-speed problems and for exploring the general aerodynamic characteristics of canard airplane configurations at supersonic speeds.

An experimental study has been conducted at supersonic speeds of some generalized airplane configurations which use canard surfaces for longitudinal control. Some of the results of this study are presented in reference 2 and include longitudinal and lateral stability characteristics obtained at Mach numbers of 1.41 and 2.01 for two canard airplane configurations having a 60° delta wing and an aspect-ratio-3 trapezoid wing. The configurations of reference 2 were selected on the basis of available information as a concept of a good supersonic airplane configuration having minimum changes in aerodynamic characteristics from subsonic to supersonic speeds. It would therefore appear desirable in obtaining subsonic information on an advanced generalized canard model to use the same configurations which were tested at supersonic speeds.

The present investigation was conducted in the Langley high-speed 7- by 10-foot tunnel with the models of reference 2. Longitudinal and lateral stability characteristics with and without the canard surface deflected were obtained over a Mach number range from 0.60 to 0.94 and a maximum angle-of-attack range from approximately -2° to 24° at the lowest test Mach number. In addition to tests of the complete model configurations, assorted breakdown tests were made to determine effects of addition of canard surfaces, the vertical tail, and the ventral fins. Some brief tests were made with a body flap and a canard flap in attempts to increase the maximum angle of attack for which the model could be trimmed in pitch.

[redacted]

SYMBOLS

Lateral stability results of this investigation are referred to the body axis system which is shown in figure 1 together with an indication of positive directions of forces, moments, and angular deflections of the model. The lift and drag characteristics presented at zero sideslip are, respectively, normal and parallel to the relative wind as shown in the side view of the model in figure 1. Moment coefficients are given about the reference center shown in figure 2 (located on the body center line at body station 25). This position corresponds to a location 17.8 percent mean aerodynamic chord ahead and 7.75 percent mean aerodynamic chord behind the leading edge of the mean aerodynamic chord for the trapezoid wing and delta wing, respectively.

C_L	lift coefficient, $\frac{\text{Lift}}{qS}$
C_D	drag coefficient, $\frac{\text{Drag}}{qS}$ at $\beta = 0^\circ$
C_D'	approximate drag coefficient at $\beta \neq 0^\circ$
C_m	pitching-moment coefficient, $\frac{\text{Pitching moment}}{qS\bar{c}}$
C_l	rolling-moment coefficient, $\frac{\text{Rolling moment}}{qSb}$
C_n	yawing-moment coefficient, $\frac{\text{Yawing moment}}{qSb}$
C_Y	lateral-force coefficient, $\frac{\text{Lateral force}}{qS}$
q	dynamic pressure, $\rho V^2/2$
V	velocity, ft/sec
ρ	air density, slugs/cu ft
M	Mach number
S	wing area (including area inside body), sq ft
b	wing span, ft

[redacted]

$\bar{c}$ wing mean aerodynamic chord (based on total area including area inside body), ft

α angle of attack of fuselage center line, deg

β angle of sideslip, deg

δ_c deflection angle of canard surface (positive with trailing edge down), deg

Subscripts:

β denotes partial derivative of a coefficient with respect to sideslip; for example, $C_{n_\beta} = \frac{\partial C_n}{\partial \beta}$

t denotes effect due to addition of vertical tail

MODEL DESCRIPTION

The basic model configurations tested are shown in figure 2 with some of the pertinent model dimensions. Details of the model geometry are given in table I and coordinates of the body are given as table II.

Two low-aspect-ratio-wing plan forms of current interest were tested on the same body to study the characteristics of two canard airplane configurations having a highly swept delta wing and a trapezoid wing of low sweep. The 60° delta wing had an aspect ratio of 2.31 and a maximum thickness of 4 percent of the wing chord. The trapezoid wing had an aspect ratio of 3, taper ratio of 0.143, and an unswept 80-percent-chord line (28.82° sweepback of the quarter-chord line). The maximum thickness of the trapezoid wing was 4 percent of the wing chord also. Both of the wings tested were made of steel and had hexagonal airfoil sections with 5° semiapex angles normal to the leading edge and normal to the trailing edge.

The canard control surface which had hexagonal airfoil sections (see fig. 3) of the same description as for the wings was remotely controlled over a deflection range from 0° to 15°.

Two auxiliary devices (see fig. 3) were studied as possible means for obtaining positive pitching-moment increments to aid the canard surface in providing trimming moments at high angles of attack. The body nose flap was a conical segment having a radius equal to the body radius

at the flap leading edge. The canard flap was a wedge which simulated a split flap deflected 30°.

The model with the trapezoid wing was modified for part of the investigation by adding a 5-inch-long cylindrical extension to the base of the original body. (See fig. 2.)

TESTS AND CORRECTIONS

Tests

The present investigation was conducted in the Langley high-speed 7- by 10-foot tunnel over a Mach number range from 0.60 to 0.94. The average test Reynolds number based on the mean aerodynamic chord was approximately 4.5×10^6 for the delta wing and 3.5×10^6 for the trapezoid wing at $M = 0.90$.

The model was mounted on a six-component internal strain-gage balance of the same description as that used in the tests of reference 2 and the balance was supported by a variable-angle sting. Longitudinal stability characteristics were investigated at zero sideslip throughout the angle-of-attack range with the Mach number and canard deflection held constant. Lateral stability derivatives of this investigation were obtained from tests conducted through the angle-of-attack range with the model at fixed sideslip angles of ±4°. The maximum range of angle of attack extended from approximately -2° to 24° at the lowest test Mach number. Some limited tests were conducted through a range of sideslip angles from -4° to 12° with the model angle of attack held constant.

Corrections

Jet-boundary corrections to the angles of attack and drag coefficients determined from reference 3 were added to the data. Blockage corrections applied to the Mach numbers were determined from reference 4. Drag coefficients have been corrected for a small tunnel-buoyancy effect and corrections have also been applied to the drag coefficients such that the base-pressure conditions correspond to free-stream static pressure.

The angles of attack and sideslip of the model have been corrected for deflection of the balance and sting under load.

RESULTS

The effect of the canard on the aerodynamic characteristics in pitch of the delta-wing model is presented in figure 4. Effects of canard deflection on the model with the delta and trapezoid wings are given in figures 5 and 6, respectively, and effects of a body nose flap and canard flap are shown in figure 7 for the model with the delta wing. The effects of the ventral fins on longitudinal characteristics for the delta-wing configuration are shown in figure 8, and effects of the 5-inch-afterbody extension for the model with the trapezoid wing are shown in figure 9.

Lateral stability derivatives of the model with the delta wing which show effects of the canard surface, canard deflection, and vertical tail are presented in figures 10 and 11. Figure 12 presents the effects of both the vertical tail and the ventral fins on the lateral stability derivatives of the trapezoid-wing configuration. Aerodynamic characteristics in sideslip showing effects of the canard surface and canard deflection are presented in figure 13 for the delta-wing configuration.

The variation with Mach number of the longitudinal and directional stability at zero lift, of minimum drag coefficient, and of maximum lift-drag ratio is presented in figure 14. Longitudinal characteristics for trim conditions throughout the lift range are given in figure 15. Pitching-moment results are presented in figure 16 and these results show effects of static margin on the control characteristics of the models. Incremental effects of the canard surface and canard deflection on lateral stability parameters for the delta-wing model are presented in figure 17. Effects of the ventral fins on overall directional stability and effects of canard deflection on the tail contribution to directional stability are shown in figure 18.

DISCUSSION

A desirable airplane arrangement would have the center of gravity located such that the full lifting capabilities of the wing can be realized in flight with the airplane trimmed at the most forward position of the center of gravity and be no less than neutrally stable with the center of gravity in the rearmost position. The canard airplane arrangement therefore should typically have a more forward center-of-gravity position than tailless or tail-rearward airplanes as a result of the destabilizing contribution of the canard surface. For example, addition of the canard surface to the present delta-wing configuration caused a destabilizing static margin shift of approximately 10 percent $\bar{c}$ (fig. 4) through the test Mach number range. The rather forward location of the reference center of gravity for the present models coincided with the

moment center used in the results for reference 2 and does not necessarily indicate an optimum center-of-gravity location which would depend on both longitudinal and directional stability and control. The results summarized in figure 14 show that the low-lift static margin was quite large for both wing plan forms at a Mach number of 0.60 and increased about 3 percent $\bar{c}$ as the Mach number increased to 0.94. The high level of longitudinal stability shown in figure 14 would be excessive for an aircraft designed to fly at supersonic as well as subsonic speeds and the moment reference would have to be shifted rearward for application of the present data to such an arrangement.

Longitudinal Stability Characteristics

Control effectiveness of the basic models.- Effects of canard deflection on the longitudinal stability characteristics of the model with the delta and trapezoid wings are presented in figures 5 and 6, respectively, and trim longitudinal characteristics obtained from figures 5 and 6 are summarized in figure 15 for the lowest and highest test Mach numbers. The results of figure 15 show that the maximum lift coefficient for which the model could be trimmed with the canard surface deflected 15° was a little greater than 0.30 at $M = 0.60$ for both wing plan forms and decreased to approximately 0.20 at $M = 0.94$.

Reasons for the low values of maximum trim lift coefficients obtained are apparent from the pitching-moment curves of figures 5 and 6 which show a relatively high static margin and the occurrence of stalling of the canard surface at the highest deflection angles. In the absence of body and wing induced upwash, the canard angle of attack would be equal to the airplane angle of attack plus the deflection angle, and, therefore, at high initial deflections, stalling of the canard surface would be expected to occur at relatively low airplane angles of attack.

In order to assess the canard control characteristics for more reasonable values of static margin, the data of figures 5 and 6 have been referred to different moment-center locations and those results are given in figure 16. The pitching moments presented in figure 16 are for low-lift static margins of 5 and 10 percent of the mean aerodynamic chord for $\delta_c = 0°$. These results show that the maximum trim lift was extended by reducing the stability; however, there was very little control effectiveness above a lift coefficient of approximately 0.7 for either the delta-wing or the trapezoid-wing model. The problem of the maximum airplane trim lift being limited by stalling of the canard was not encountered in the tests at supersonic speeds (ref. 2) because of the beneficial effects of supersonic Mach number on maximum lift characteristics. It appears, therefore, that for a configuration having a small transonic aerodynamic-center shift, the problem of canard control effectiveness will lie primarily in the subsonic region rather than supersonic.

[redacted]

A comparison of pitching-moment results for the delta-wing and trapezoid-wing models presented in figures 5 and 6 shows some differences which should be explained. The values of pitching moment at zero lift (figs. 5 and 6) show that a larger pitching-moment coefficient was produced by a given control deflection on the trapezoid-wing model than for the delta-wing model. When interference is neglected, the canard surface should be expected to provide the same moment regardless of which wing is behind it, and this moment should trim the configuration having the lowest static margin to the higher trim-lift value. The two wing plan forms had the same area; however, the mean aerodynamic chord for the delta wing was approximately 28 percent greater than that for the trapezoid wing, and this difference is reflected in the differences in canard effectiveness at zero lift and in the canard contribution to longitudinal stability. Not all the differences in control effectiveness and maximum trim lift can be attributed to differences in the reference length used in the coefficients; however, most of the differences shown for the two wing plan forms can be attributed to this source.

Auxiliary control devices.- Several means have been studied in the past for increasing the lifting capabilities of canard surfaces at low speeds such as addition of leading-edge slats and various types of trailing-edge flaps. (See ref. 1.) These devices and recent developments in the use of boundary-layer control offer promising means for materially increasing the lifting capabilities of a canard surface at low speeds. Another approach to the problem of attaining trim at high lift coefficients is that of relieving the canard surface of the bulk of the moments to be trimmed by use of auxiliary trimming devices. Some limited test results were obtained with a body flap (shown in fig. 3) used as a device to provide a positive pitching-moment increment. Test results obtained with this flap for the delta-wing model (fig. 7) at a Mach number of 0.60 show that an appreciable increment in pitching-moment coefficient resulted from the addition of the flap. Near zero lift, this increment was approximately equal to the increment which would be obtained with the basic canard surface deflected 7°. The maximum lift coefficient at which the model could be trimmed with a canard surface deflected 10° was increased from 0.30 to 0.55 by addition of the body flap. A benefit of the body flap, in addition to the basic increment at zero lift, was the increase in control effectiveness at high lift coefficients. The drag increment of the body flap shown in figure 7 suggests that it would be suited only as an aid in trimming for low-speed flight.

In addition to the body flap, some results were obtained with a 30° wedge attached to the canard surface as shown in figure 3 which simulated a split flap deflected 30°. Addition of this simulated canard flap provided appreciable gains in trim lift coefficient (fig. 7) over the basic arrangement; however, this flap was much less effective than the body flap. Of course much more effective canard flap arrangements are

possible, such as a single or double slotted flap; however, all these devices load the canard more heavily rather than provide a trimming moment that would be independent of the canard.

Effect of ventral fins and extended afterbody.- Effects of the ventral fins on the longitudinal characteristics at the lowest and highest test Mach number are given in figure 8 and show essentially no effect of the ventral fins on the longitudinal stability of the delta-wing model. The lack of appreciable effects of the ventral fins on either longitudinal or directional stability (fig. 18) probably results from the fact that the center of area of the ventral fins is located close to the moment reference.

Tests were made with an extended afterbody on the trapezoid-wing configuration in order to establish the subsonic stability level for an evaluation of effects of afterbody extension on the aerodynamic-center shift in going from subsonic to supersonic speeds. The present tests showed essentially no effect of the afterbody extension on longitudinal stability at low and moderate lift coefficients. (See fig. 9.)

Lateral Stability Characteristics

Effects of canard surface and canard deflection on lateral stability derivatives.- Effects of addition of the canard surface and canard deflection on the static lateral stability derivatives of the delta-wing model are presented in figure 10 and increments obtained from figure 10 are summarized in figure 17 for a Mach number of 0.60. These results show very little effect on directional stability of adding the canard surface at 0° deflection at low and moderate angles of attack. For angles of attack greater than 15° at $M = 0.60$, the directional stability was slightly higher with the canard surface on. Deflection of the canard surface to 10° had little effect on directional stability up to an angle of attack of 6°; however, above this angle of attack, significant increases in directional stability occurred when the deflection was increased from 0° to 10°. (See fig. 17.) Addition of the canard surface caused large negative increments in C_{l_β} to occur at moderate and high angles of attack with the maximum effect occurring at 15°. The results of figure 17 indicate furthermore that these effects due to addition of the canard surface were associated with interaction on the wing rather than on the vertical tail inasmuch as negative increments in C_{l_β} would not be expected to accompany positive increments of C_{Y_β} which came from a vertical tail located above the roll reference axis.

The tail-off results presented in figures 11 and 12 show that some of the beneficial effects of deflecting the canard surface at moderate

[redacted]

angles of attack can be attributed to a small reduction in the instability of the wing-body-canard configuration. Even with the canard surface undeflected, a small reduction in instability with increasing angle of attack occurred with the delta-wing configuration, and the trapezoid-wing model became directionally stable without the tail at high angles of attack (fig. 12). These tail-off characteristics do not follow the trends encountered on many swept-wing—body configurations which generally show substantial increases in directional instability at moderately high angles of attack. (For example, see refs. 5 and 6.) The tail-off directional stability characteristics of the present models are believed to be appreciably influenced by two favorable effects not generally present on conventional arrangements. One of these configuration effects is the absence of an afterbody behind the wing inasmuch as reference 6 shows a favorable effect of removing the afterbody of a swept-wing—body arrangement. The other favorable effect is believed to occur at the nose of the model and is manifested by a "strake effect" of the canard surface. The strake effect was found in reference 7 from small horizontal strakes on a body nose which altered the forebody flow sufficiently to make a highly unstable swept-wing—body arrangement become directionally stable at high angles. The small favorable effect of canard deflection for the tail-off configuration (figs. 11 and 12, $M = 0.60$) appears to be further manifestation of the strake effect as indicated by the occurrence of positive increments in both C_{n_β} and C_{Y_β} with positive increments in control deflection.

The largest favorable effect of canard deflection was on the tail contribution to directional stability which is summarized in figure 18. These results show that gains attributable to canard deflection were realized for both wing plan forms and that the gains were much more pronounced for the delta-wing model which had a greater tail contribution at high angles of attack with the canard surface deflected 10° than at zero angle of attack. On the other hand, the tail contribution to directional stability with the trapezoid wing decreased rapidly with angle of attack and became negative at high angles. Reasons for the differences in variations of tail contributions with angle of attack for the two wing plan forms have not been established; however, it is possible that relatively minor differences in geometry, such as wing root leading-edge location on the body or exposed root chord length, had an important effect on the flow at the vertical tail.

The experimental directional stability results of the present study at high subsonic speeds are in general agreement with low-speed results obtained in the past in force tests in the Langley free-flight tunnel. (For example, see ref. 8 which presents results for a canard model having a 60° delta wing.) The results of reference 8 demonstrate that adding a canard surface deflected 15° has a favorable effect on the tail-off configuration and also increases the vertical-tail contribution to the directional stability at low and moderate angles of attack.

[redacted]

Effect of canard surface and canard deflection on aerodynamic characteristics in sideslip.- Aerodynamic characteristics of the delta-wing model with and without the canard surface are given in figure 13 for angles of attack of approximately 0° and 12.5° and for a Mach number of 0.60. The only significant effects of the canard surface or canard deflection for an angle of attack of approximately 0° was a nose-up pitching moment and an increase in effective dihedral which accompanied a canard deflection of 10°. At an angle of attack approximately 12.5°, an appreciable nonlinear variation of rolling-moment coefficient with sideslip angle occurred when the canard surface was off. This fact indicated that a region of negative effective dihedral existed between angles of sideslip of ±1°. Addition of the canard caused the variation to become linear up to 4° and gave the large negative increment in C_{l_β} also shown in the derivatives of figure 17.

The variation of lift, drag, and pitching-moment coefficients with sideslip presented in figure 13 shows little change in lift and drag; however, at an angle of attack of approximately 12.5°, the configuration with the canard surface deflected 10° showed a moderate variation of pitching-moment coefficient with sideslip angle.

SUMMARY OF RESULTS

The results of an investigation at high subsonic speeds of the static longitudinal and lateral stability characteristics of two canard airplane configurations are summarized in the following observations:

1. The longitudinal control characteristics indicated that stalling of the canard surface at high deflection angles (10° to 15°) occurred at relatively low model angles of attack which could impose appreciable limitations on the maximum trim lift coefficient attainable for a longitudinally stable configuration.

2. Significant improvements in control effectiveness and maximum value of trim lift coefficient were obtained from addition of a body flap having a conical shape, located slightly behind the canard on the bottom of the body.

3. Addition of the canard surface at 0° deflection had little effect on overall directional stability of the delta-wing model, whereas deflection of the canard surface to 10° had a large favorable effect on directional stability at high angles of attack for both the trapezoid- and delta-wing configurations tested.

4. There were marked differences in overall directional stability of the delta-wing and trapezoid-wing models with the canard surface deflected 10°. Directional stability of the delta-wing model was greater at high angles of attack than at the lowest angles, whereas the complete model with the trapezoid wing became directionally unstable at a moderately high angle in spite of the aforementioned benefits of canard deflection.

Langley Aeronautical Laboratory,
National Advisory Committee for Aeronautics,
Langley Field, Va., September 17, 1957.

[redacted]

REFERENCES

1. Johnson, Joseph L., Jr.: A Study of the Use of Various High-Lift Devices on the Horizontal Tail of a Canard Airplane Model as a Means of Increasing the Allowable Center-of-Gravity Travel. NACA RM L52K18a, 1953.

2. Driver, Cornelius: Longitudinal and Lateral Stability and Control Characteristics of Two Canard Airplane Configurations at Mach Numbers of 1.41 and 2.01 . NACA RM L56L19, 1957.

3. Gillis, Clarence L., Polhamus, Edward C., and Gray, Joseph L., Jr.: Charts for Determining Jet-Boundary Corrections for Complete Models in 7- by 10-Foot Closed Rectangular Wind Tunnels. NACA WR L-123, 1945. (Formerly NACA ARR L5G31.)

4. Herriot, John G.: Blockage Corrections for Three-Dimensional-Flow Closed-Throat Wind Tunnels, With Consideration of the Effect of Compressibility. NACA Rep. 995, 1950. (Supersedes NACA RM A7B28.)

5. Few, Albert G., Jr.: Investigation at High Subsonic Speeds of the Static Lateral and Directional Stability and Tail-Loads Characteristics of a Model Having a Highly Tapered Swept Wing of Aspect Ratio 3 and Two Horizontal-Tail Positions. NACA RM L56E29, 1956.

6. Polhamus, Edward C., and Spreemann, Kenneth P.: Subsonic Wind-Tunnel Investigation of the Effect of Fuselage Afterbody on Directional Stability of Wing-Fuselage Combinations at High Angles of Attack. NACA TN 3896, 1956.

7. Sleeman, William C., Jr.: Investigation at High Subsonic Speeds of the Effects of Various Horizontal Fuselage Forebody Fins on the Directional and Longitudinal Stability of a Complete Model Having a 45° Sweptback Wing. NACA RM L56J25, 1957.

8. Bates, William R.: Low-Speed Static Lateral Stability Characteristics of a Canard Model Having a 60° Triangular Wing and Horizontal Tail. NACA RM L9J12, 1949.

TABLE I.- GEOMETRIC CHARACTERISTICS OF MODEL

Body:	
Maximum diameter, in.	3.50
Length, in.	37.00
Base area, sq in.	9.582
Fineness ratio	10.57
Trapezoid wing:	
Span, in.	25.72
Chord at body-wing intersection, in.	13.25
Area, sq ft	1.53
Aspect ratio	3
Taper ratio	0.143
Thickness ratio	0.04
Mean geometric chord, in.	10.184
Sweep angle of leading edge, deg	38.67
Sweep angle of trailing edge, deg	-11.3
Leading-edge half-angle, normal to L.E., deg	5
Trailing-edge half-angle, normal to T.E., deg	5
Delta wing:	
Span, in.	22.56
Chord at body-wing intersection, in.	16.51
Mean geometric chord, in.	13.027
Area, sq ft	1.53
Aspect ratio	2.31
Thickness ratio	0.036
Leading-edge half-angle, normal to L.E., deg	5
Trailing-edge half-angle, normal to T.E., deg	5
Canard:	
Area (total to body center line), sq in.	25.354
Area, exposed (each canard), sq in.	6.742
Span, exposed, in.	2.25
Mean geometric chord, in.	3.33
Ratio of total canard area to total wing area	0.115
Vertical tail:	
Area, exposed, sq ft	0.279
Span, exposed, in.	4.25
Aspect ratio	0.439
Sweep of leading edge, deg	70
Section	3/16-in. slab
Leading-edge half-angle, normal to L.E., deg	5
Ventral fins:	
Area, each fin, exposed, sq ft	0.13
Span, exposed, in.	2.25
Aspect ratio	0.271
Sweep of leading edge, deg	60
Sweep of trailing edge, deg	-77.5
Leading-edge half-angle, normal to L.E., deg	5
Trailing-edge half-angle, normal to T.E., deg	5

[redacted]

TABLE II.- COORDINATES OF BODY

Body station	Radius	
0	0	
.297	.076	
.627	.156	
.956	.233	
1.285	.307	
1.615	.378	
1.945	.445	
2.275	.509	
2.605	.573	
2.936	.627	
3.267	.682	
3.598	.732	
3.929	.780	
4.260	.824	
4.592	.865	
4.923	.903	
5.255	.940	
5.587	.968	
5.920	.996	
6.252	1.020	
6.583	1.042	Conical
18.648	1.75	section
37.000	1.75	

[redacted]

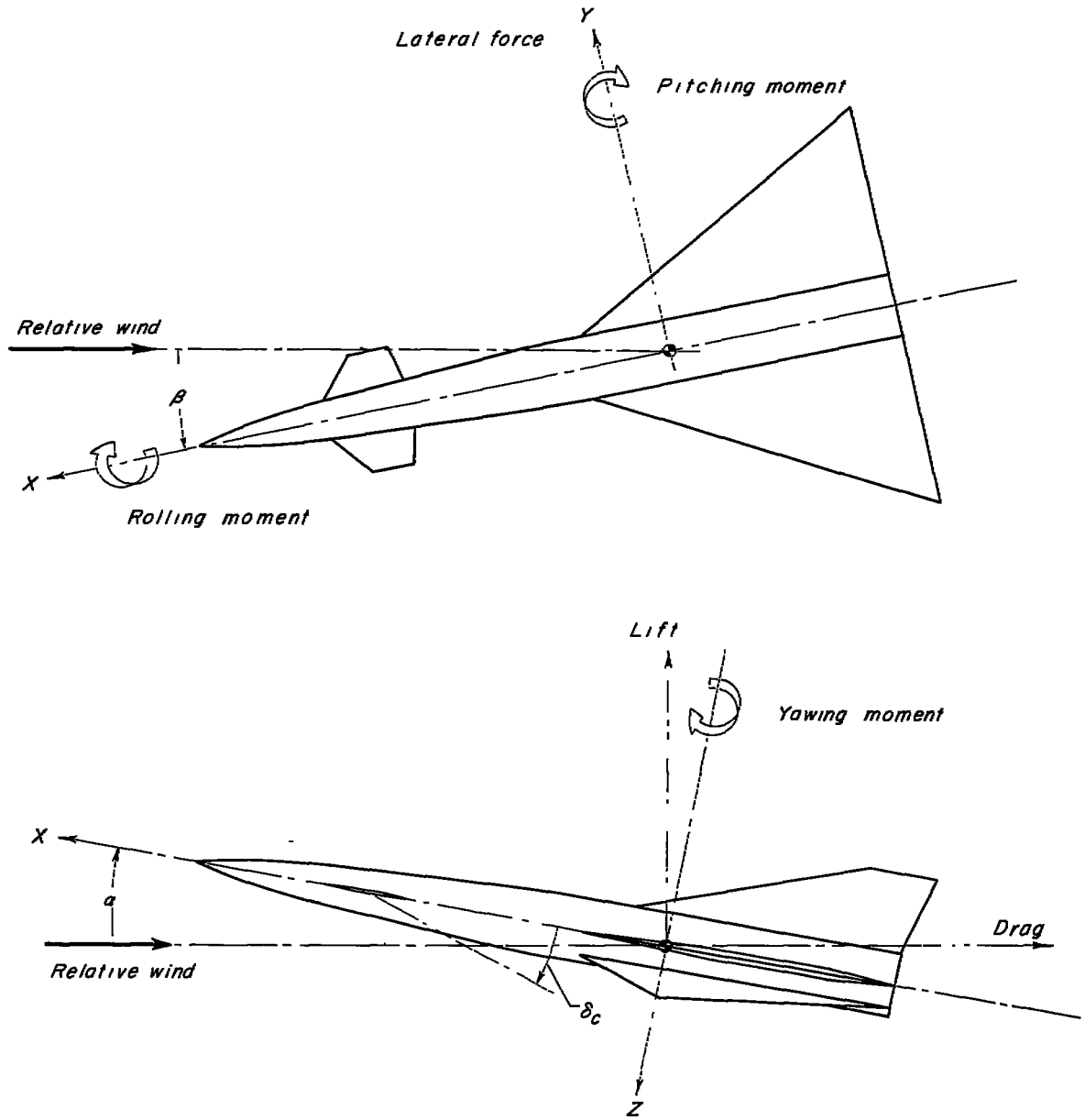

Figure 1.- Body reference axes showing positive directions of forces, moments, and angular deflections.

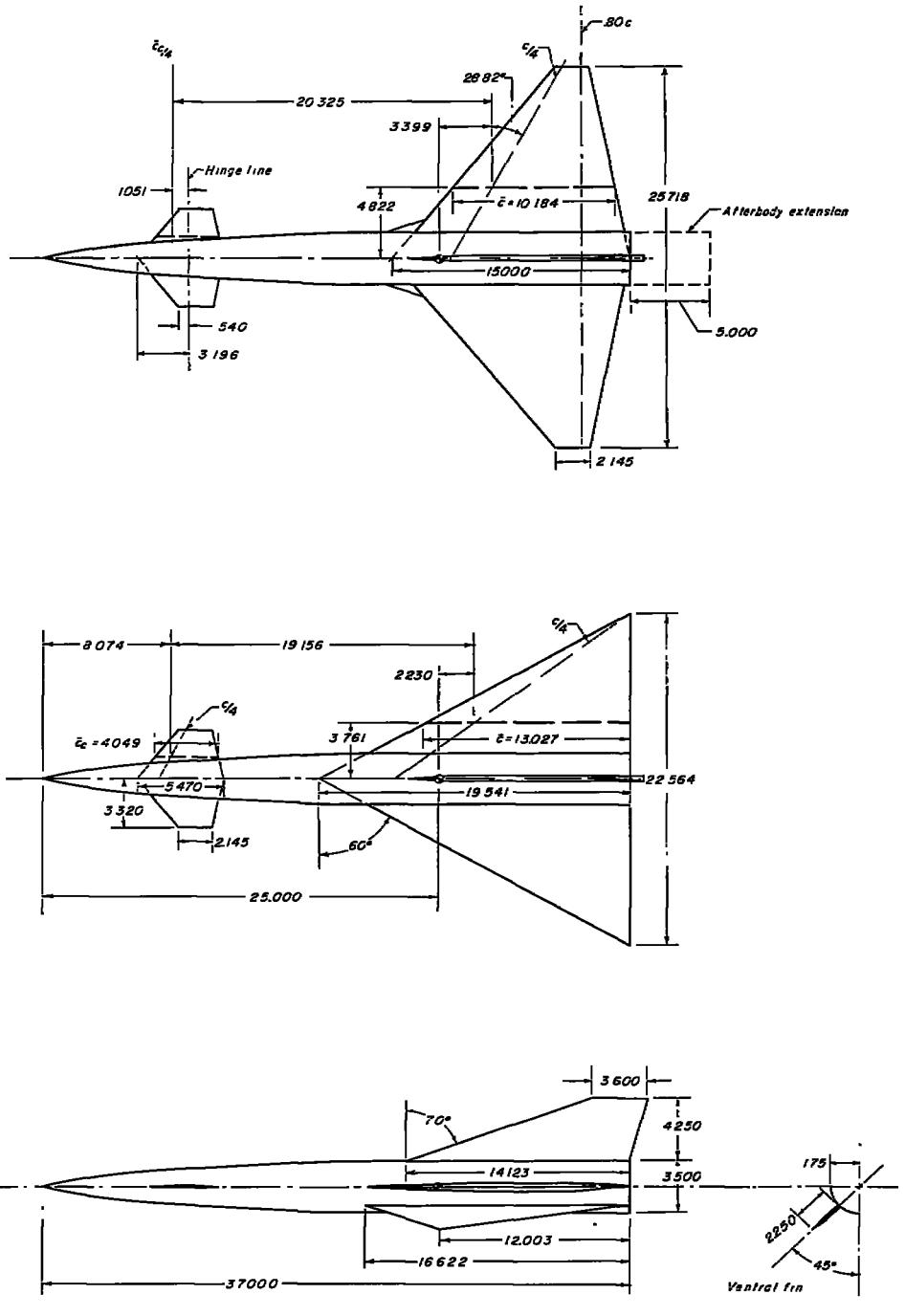

Figure 2.- General arrangement of the basic model configuration showing the delta-wing and trapezoid-wing plan forms tested. (All dimensions are in inches.)

[redacted]

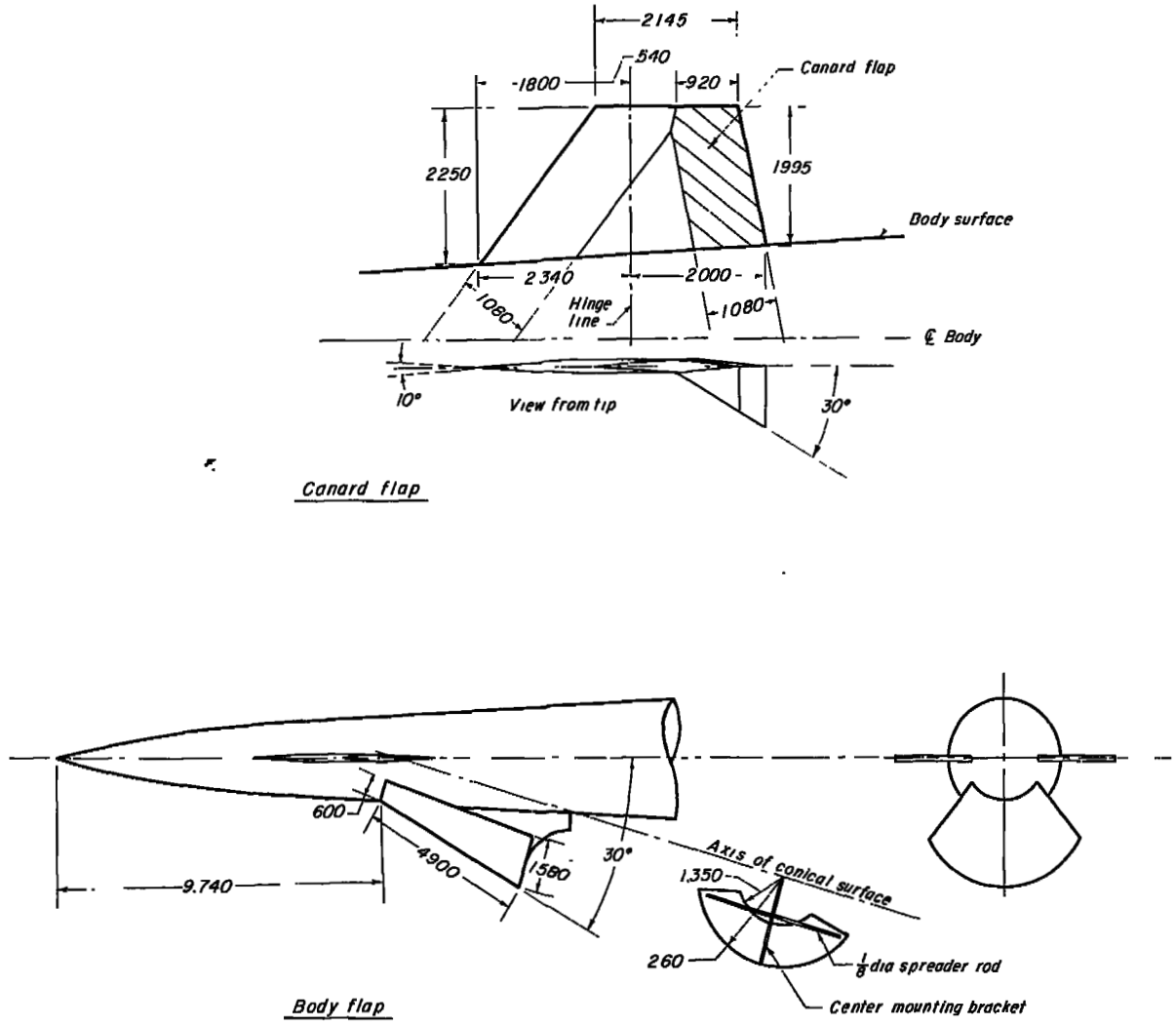

Figure 3.- Details of the body nose flap and simulated canard split flap tested on the model with the delta wing.

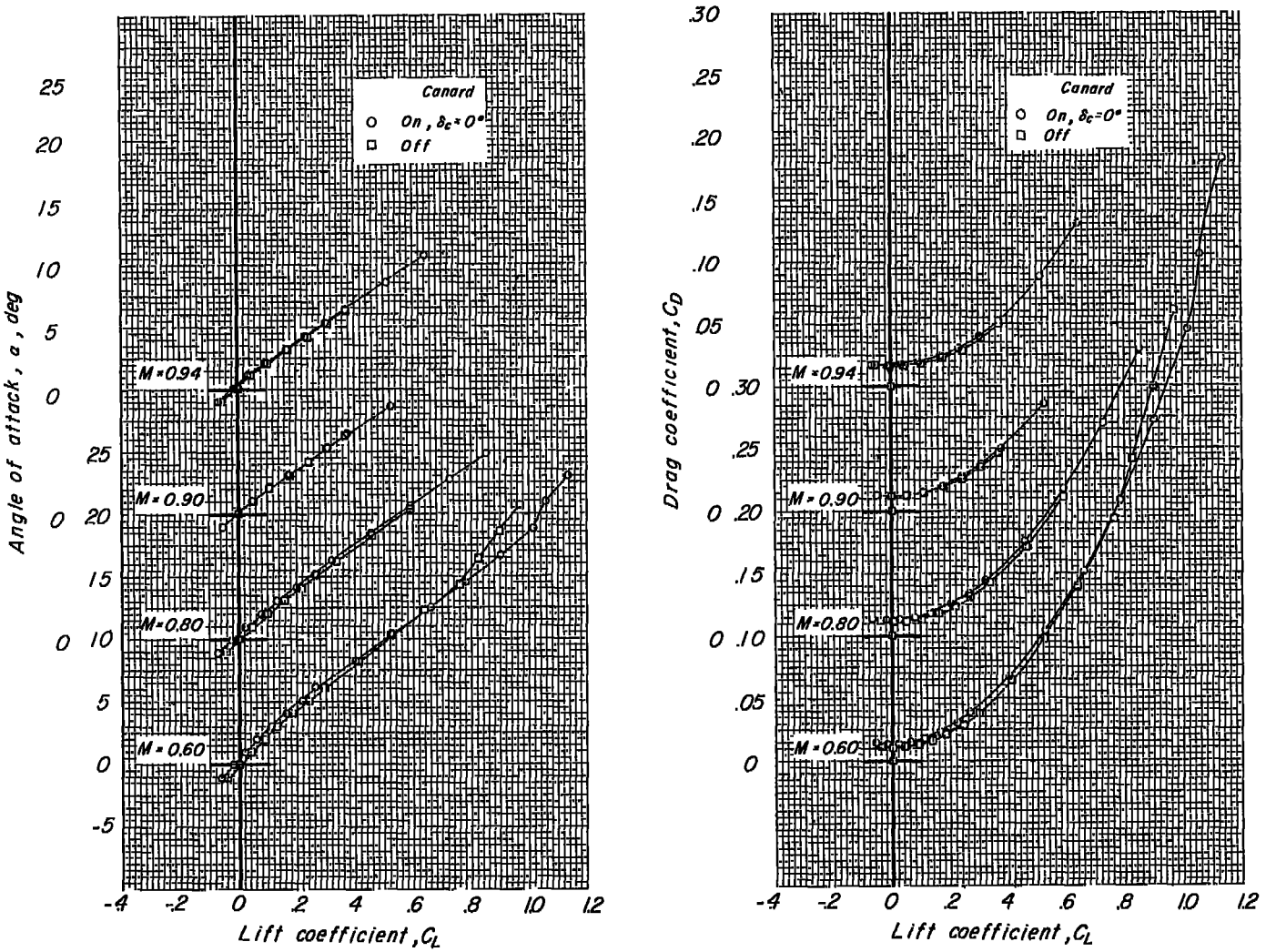

Figure 4.- Effect of the canard surface on the longitudinal characteristics of the delta-wing configuration.

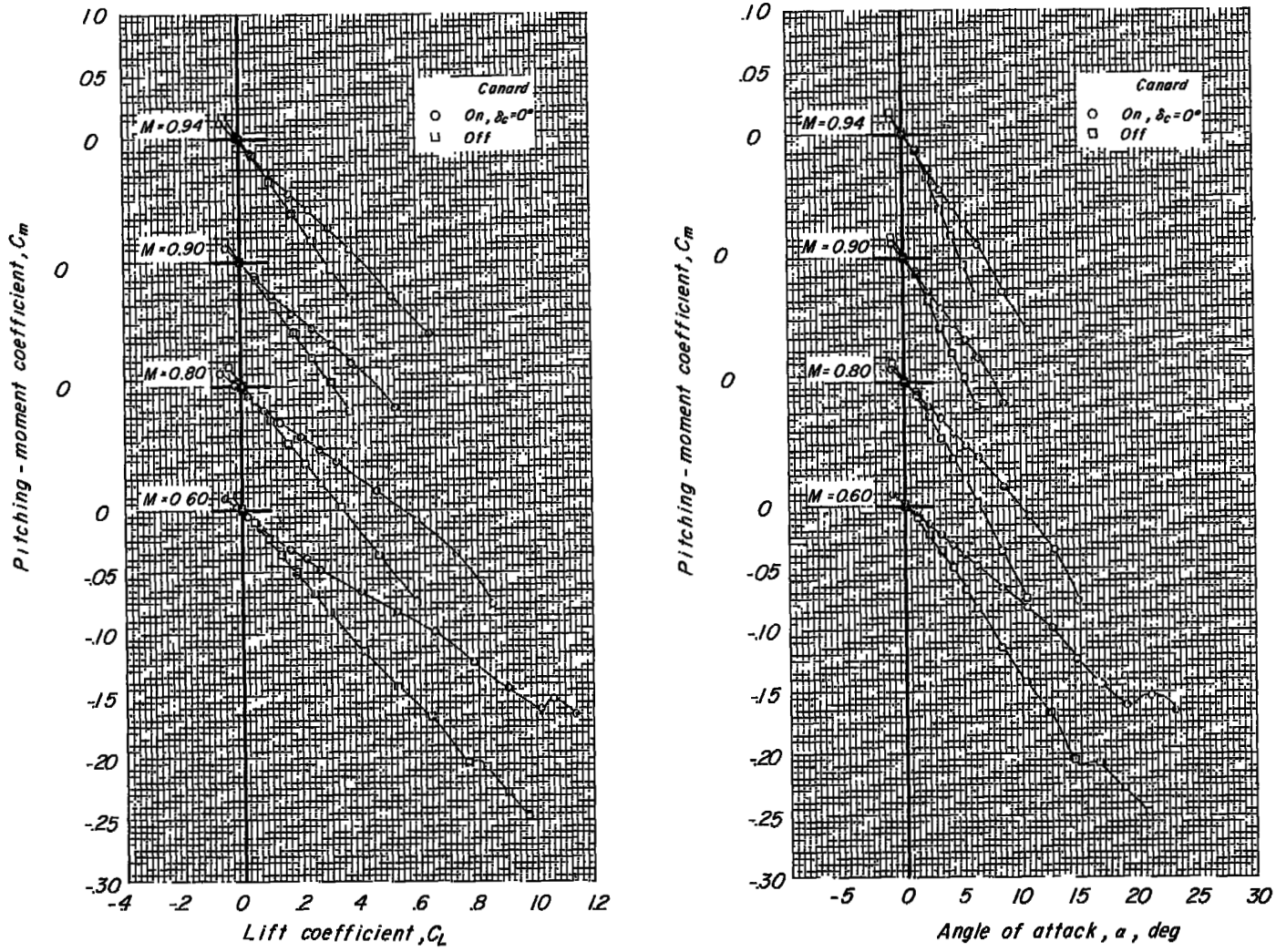

Figure 4.- Concluded.

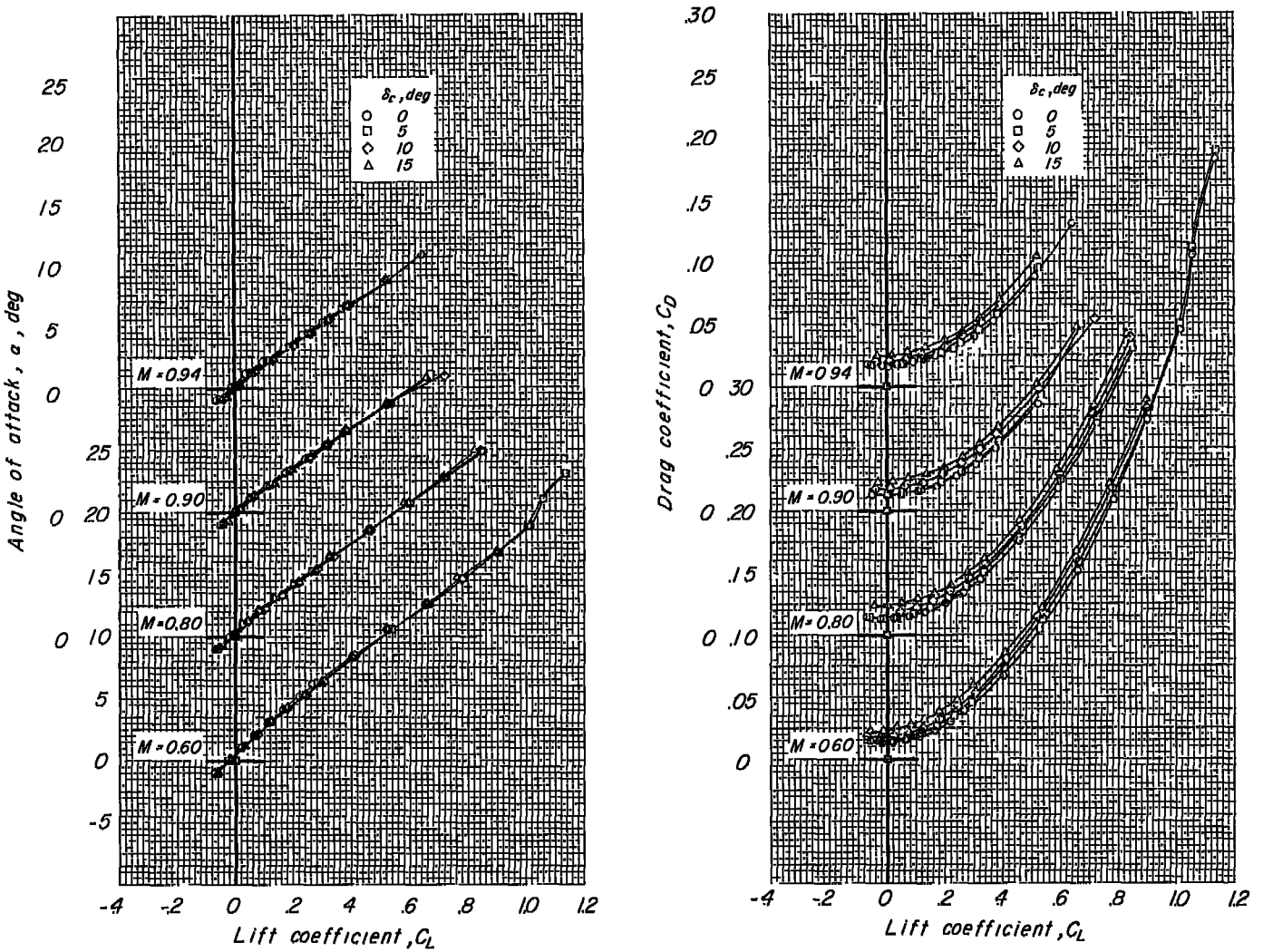

Figure 5.- Effect of canard deflection on the longitudinal characteristics of the delta-wing configuration.

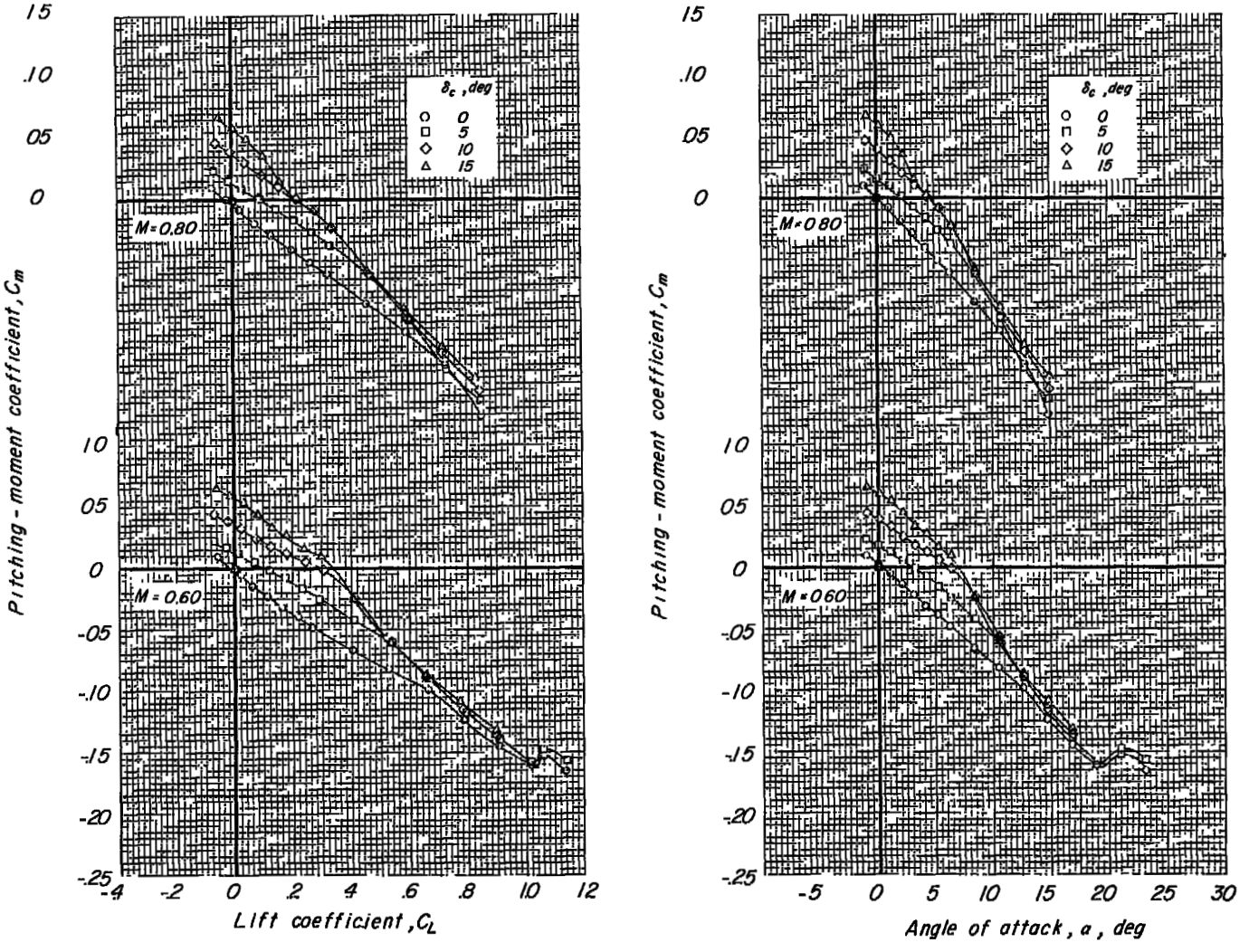

Figure 5.- Continued.

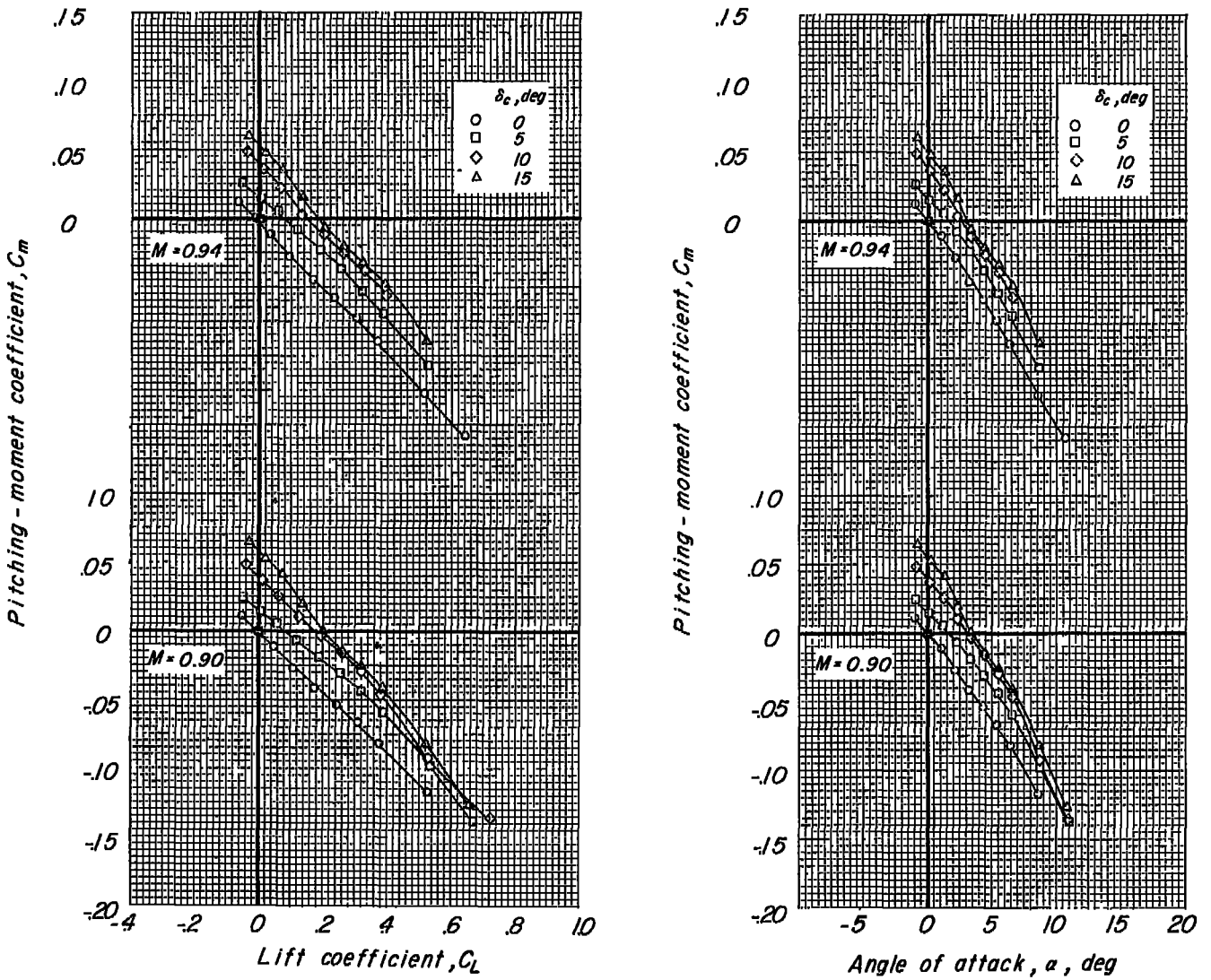

Figure 5.- Concluded.

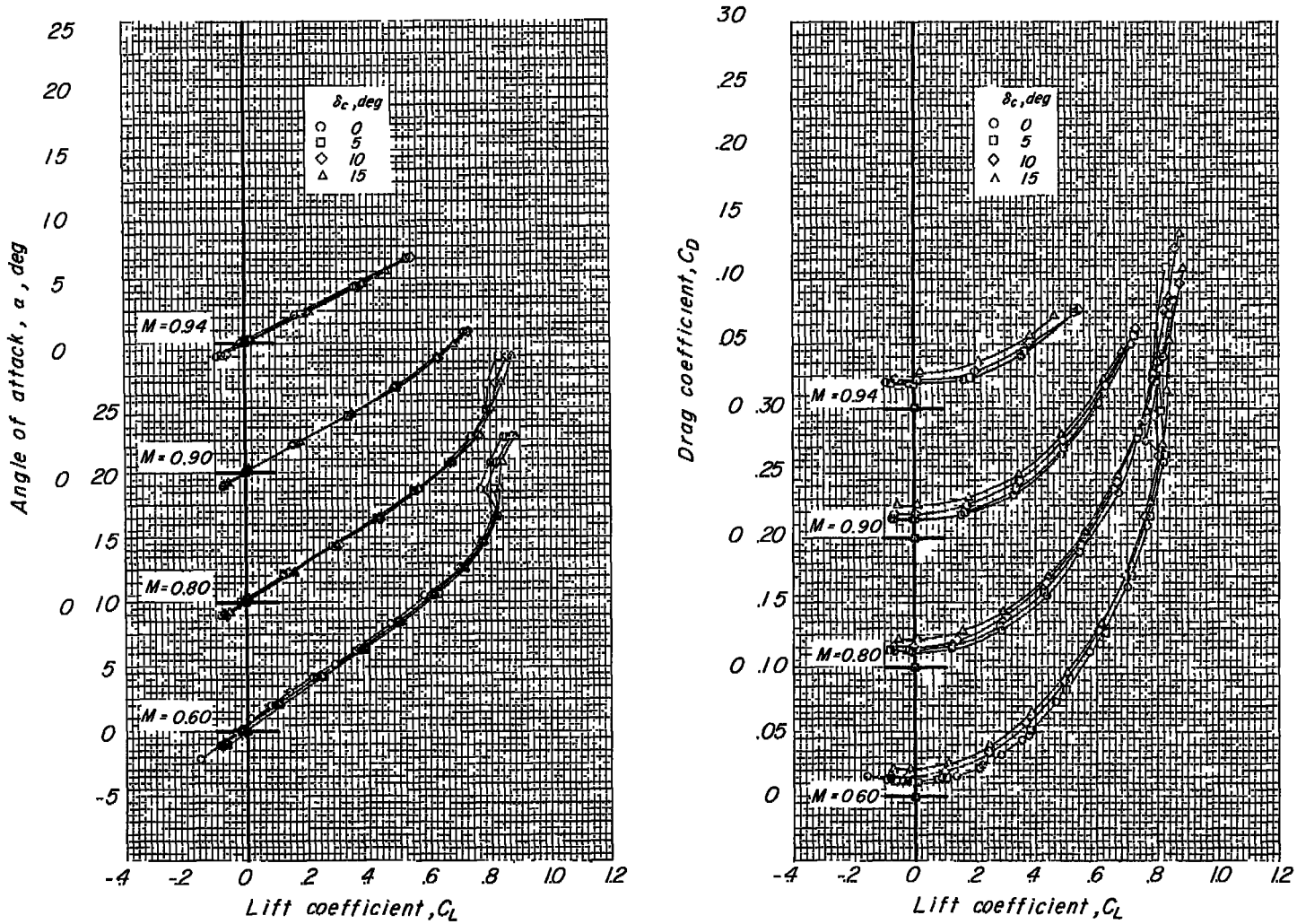

Figure 6.- Effect of canard deflection on the longitudinal characteristics of the trapezoid-wing configuration.

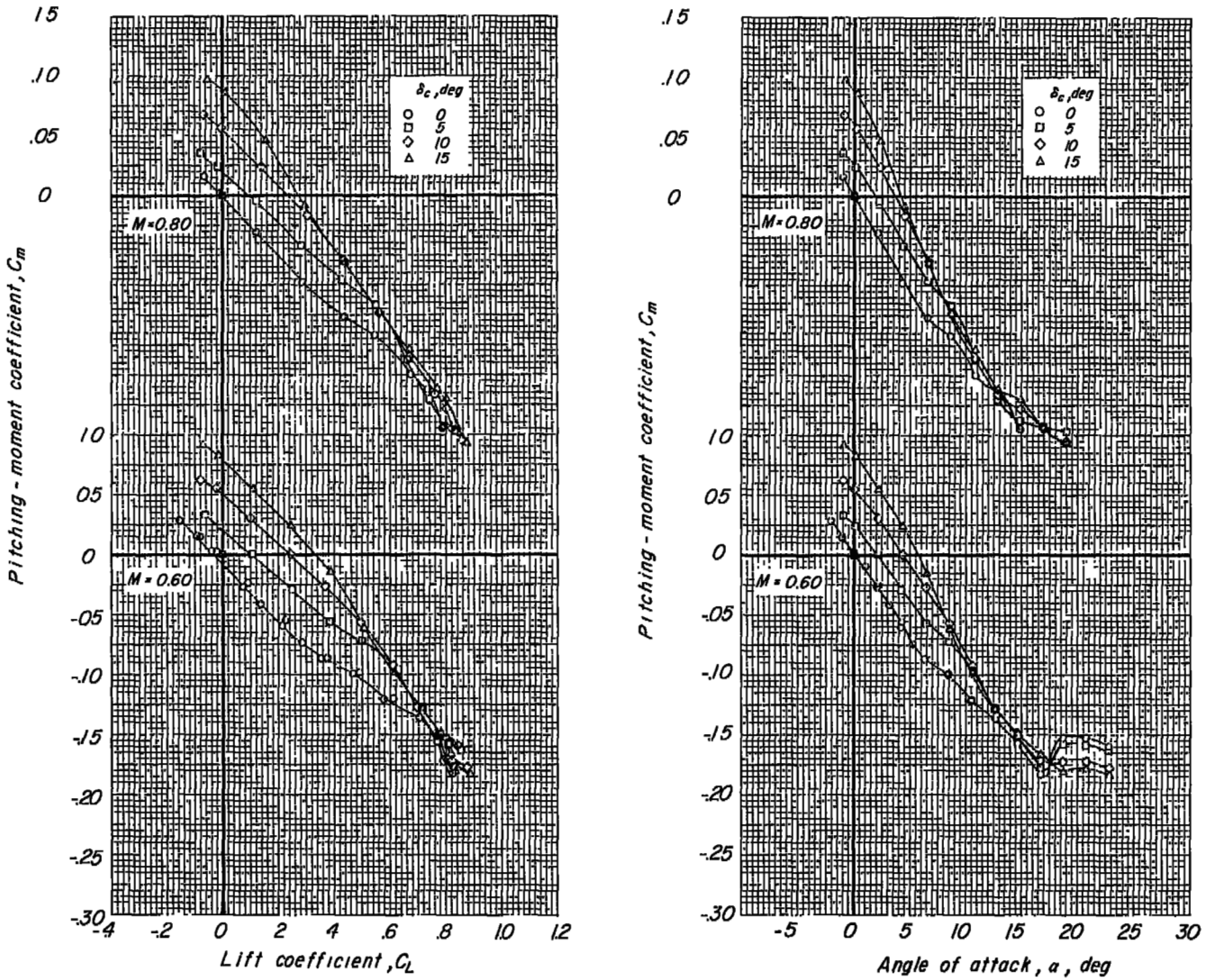

Figure 6.- Continued.

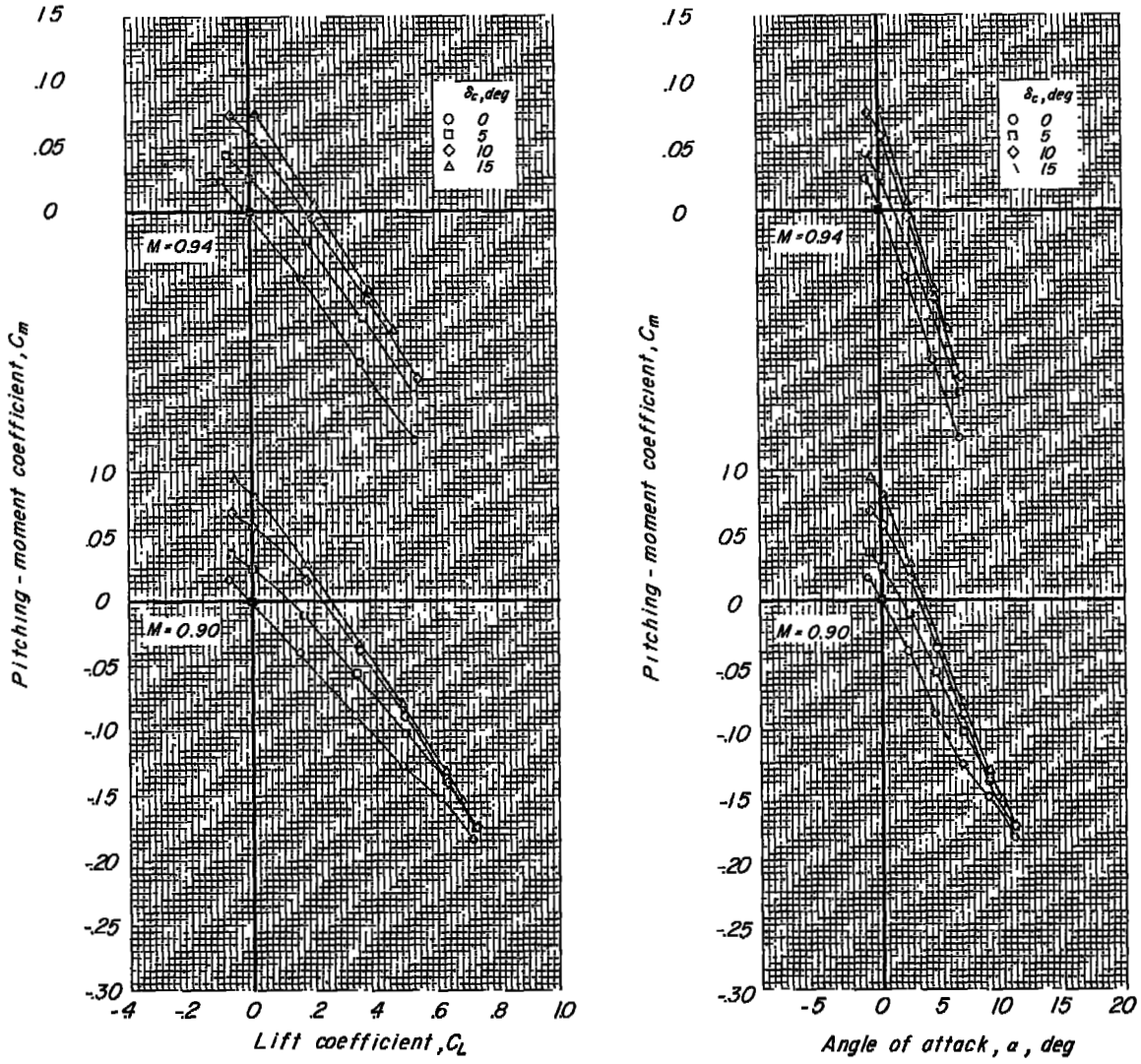

Figure 6.- Concluded.

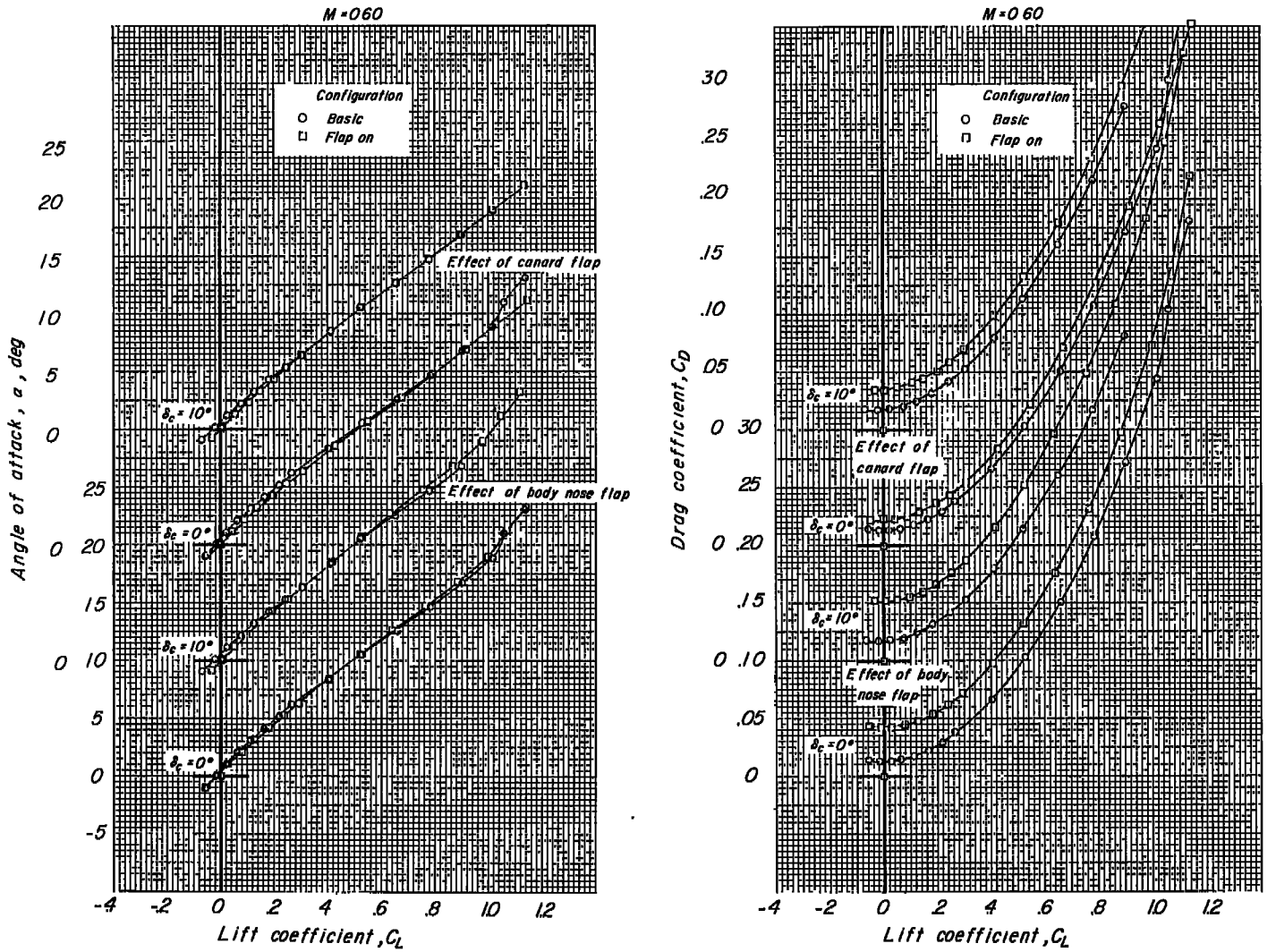

Figure 7.- Effect of body nose flap and canard flap on the longitudinal characteristics of delta-wing configuration. M = 0.60.

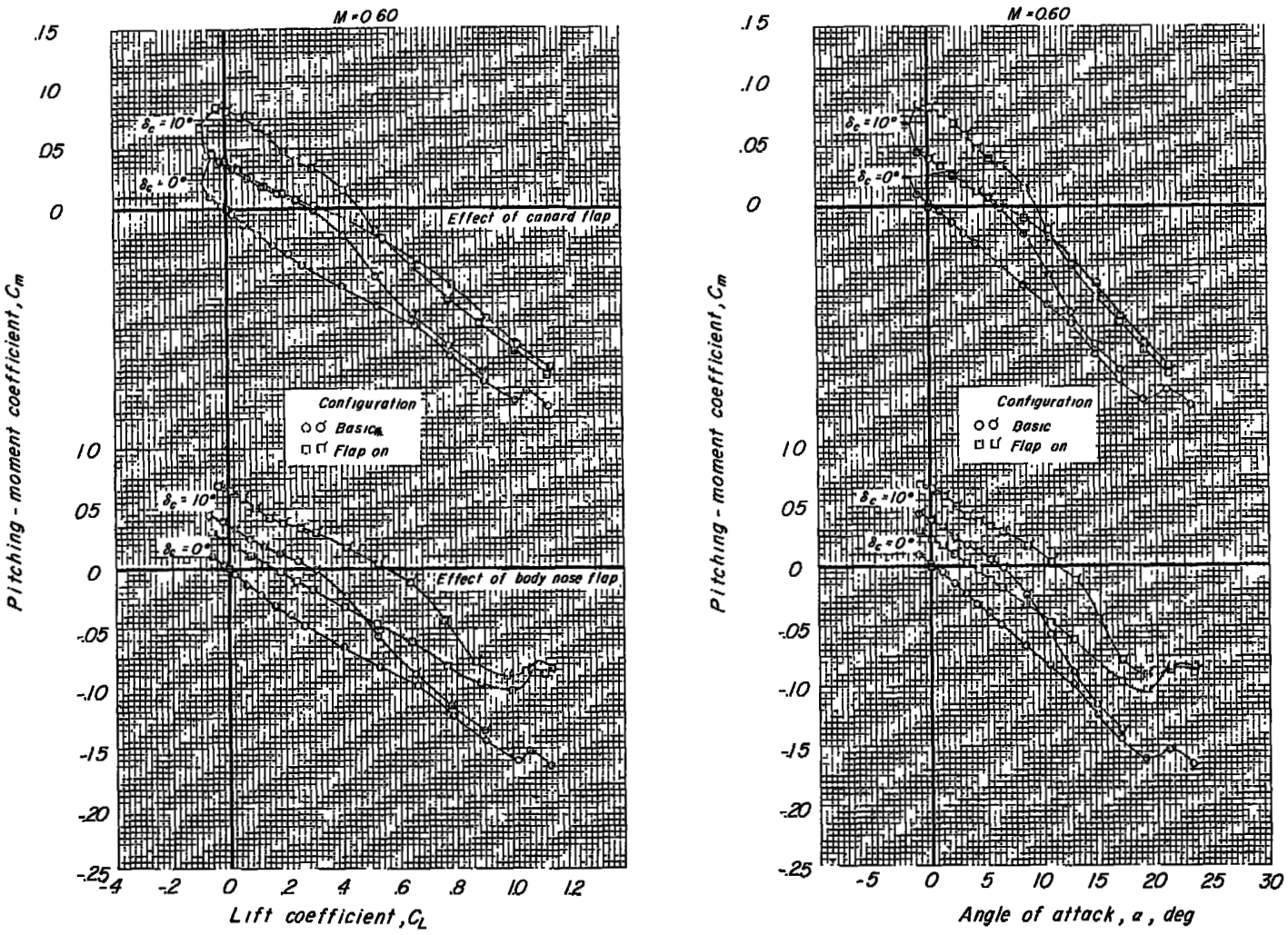

Figure 7.- Concluded. (Flagged symbols indicate $\delta_c = 10^o$.)

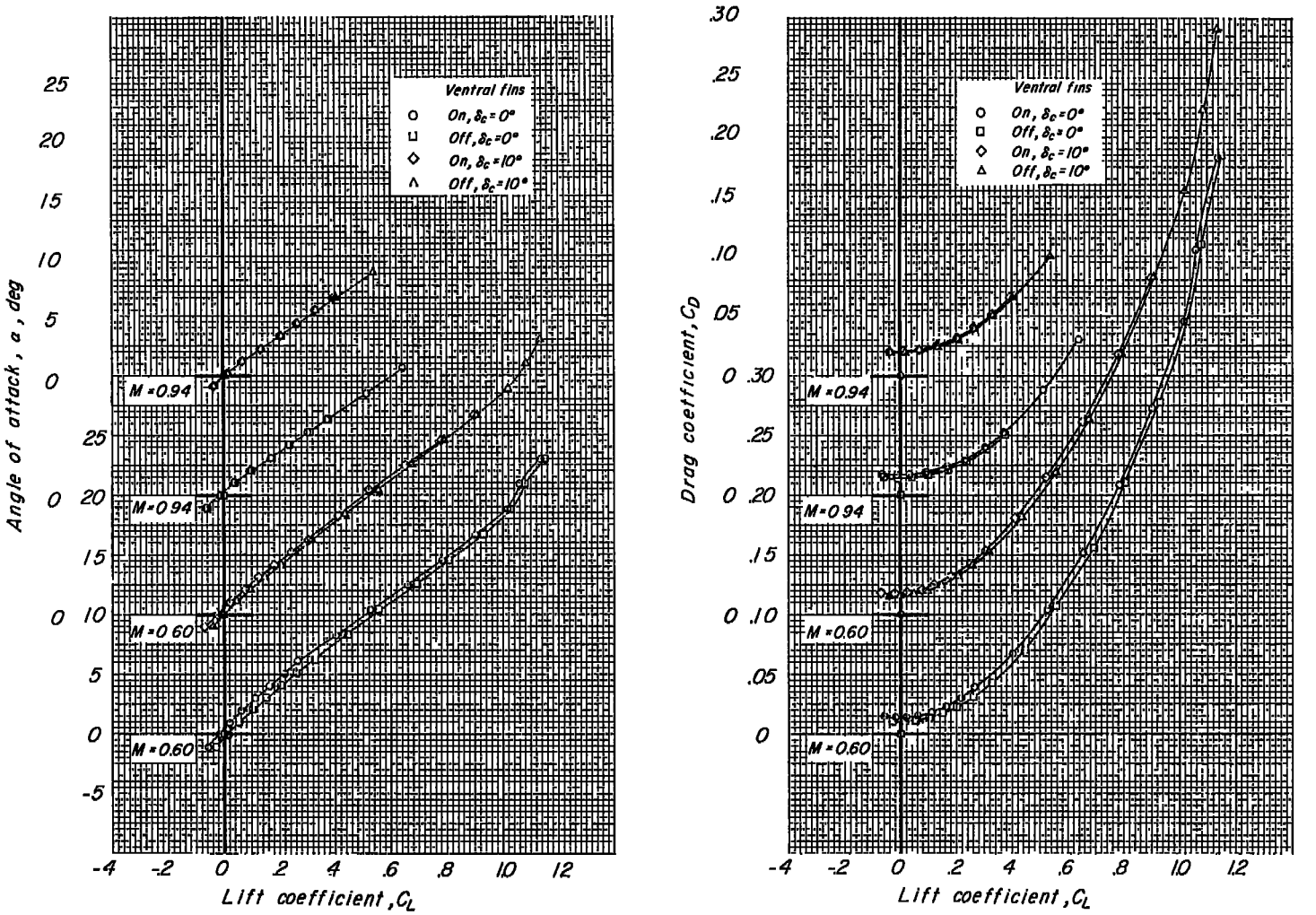

Figure 8.- Effect of the ventral fins on the longitudinal characteristics of the delta-wing configuration.

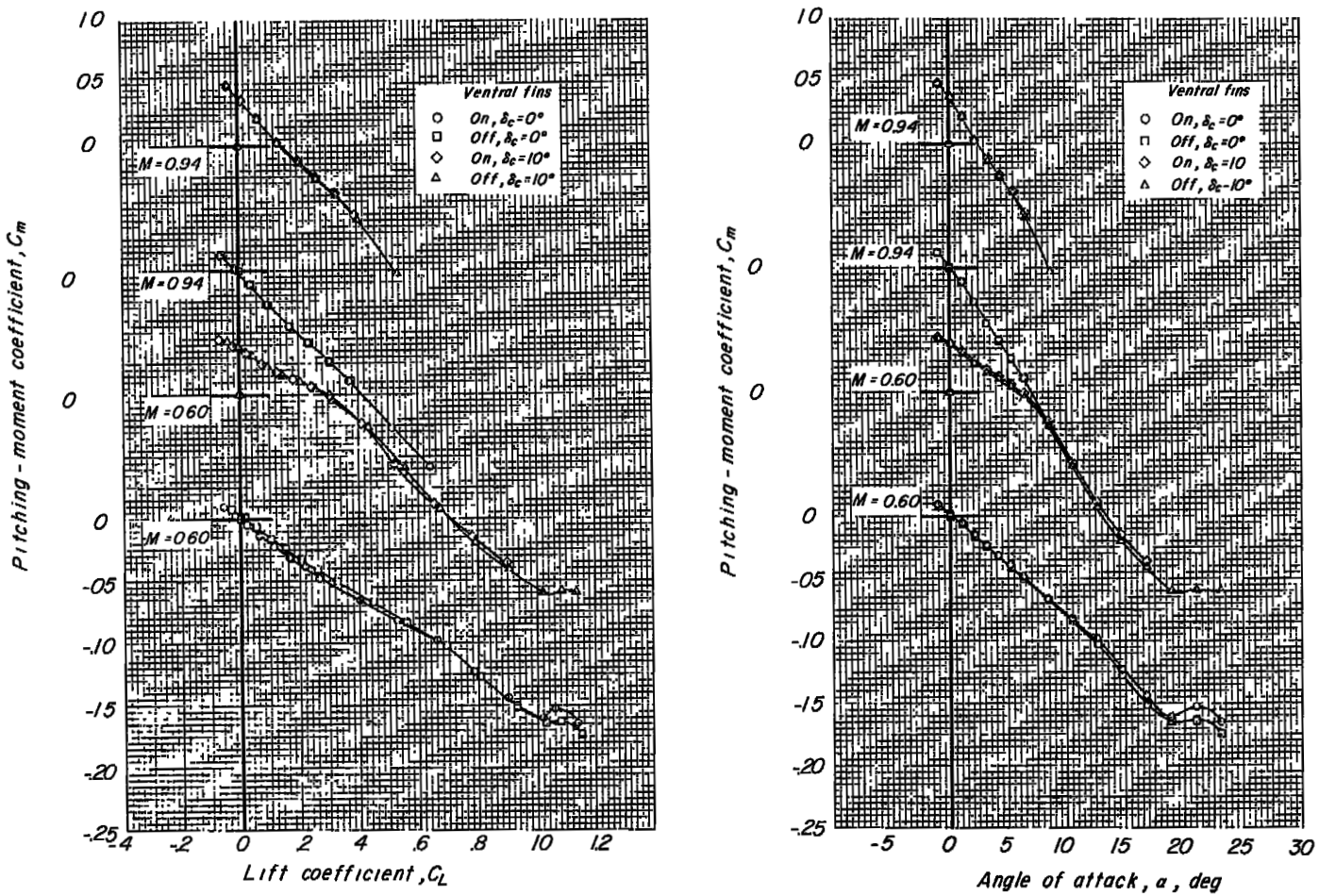

Figure 8.- Concluded.

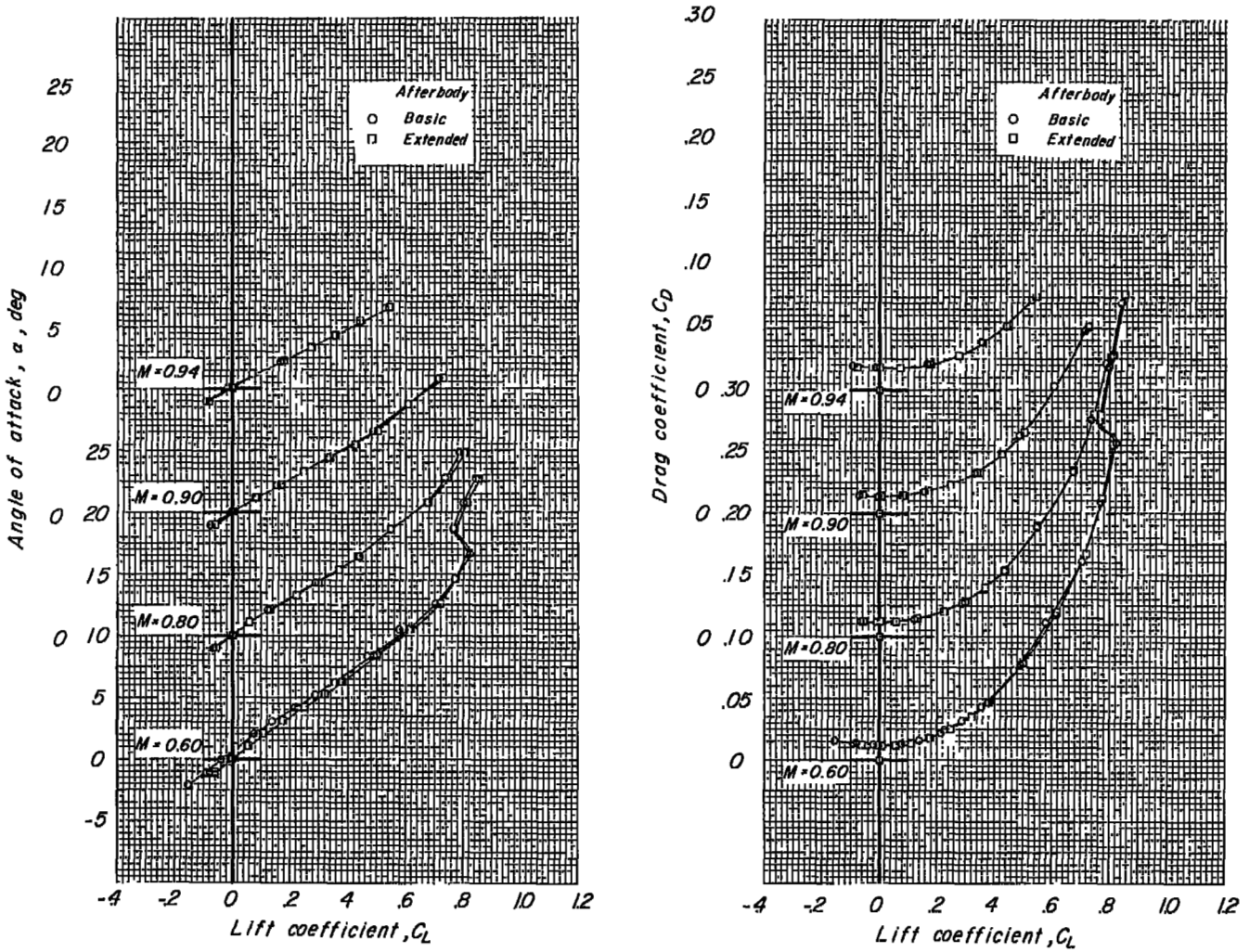

Figure 9.- Effect of 5-inch extension of the fuselage afterbody on the longitudinal characteristics of the trapezoid-wing configuration. $\delta_c = 0^\circ$.

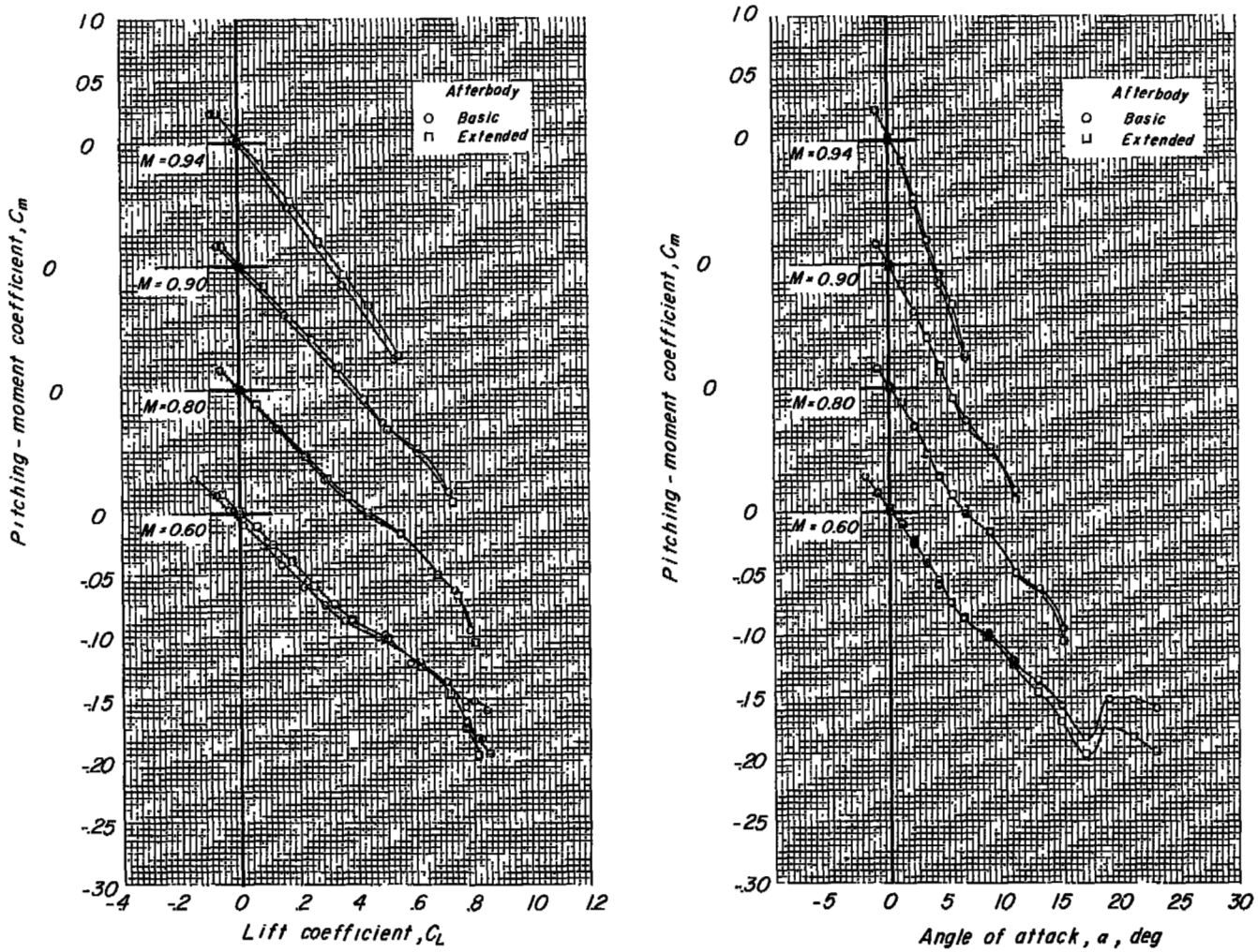

Figure 9.- Concluded.

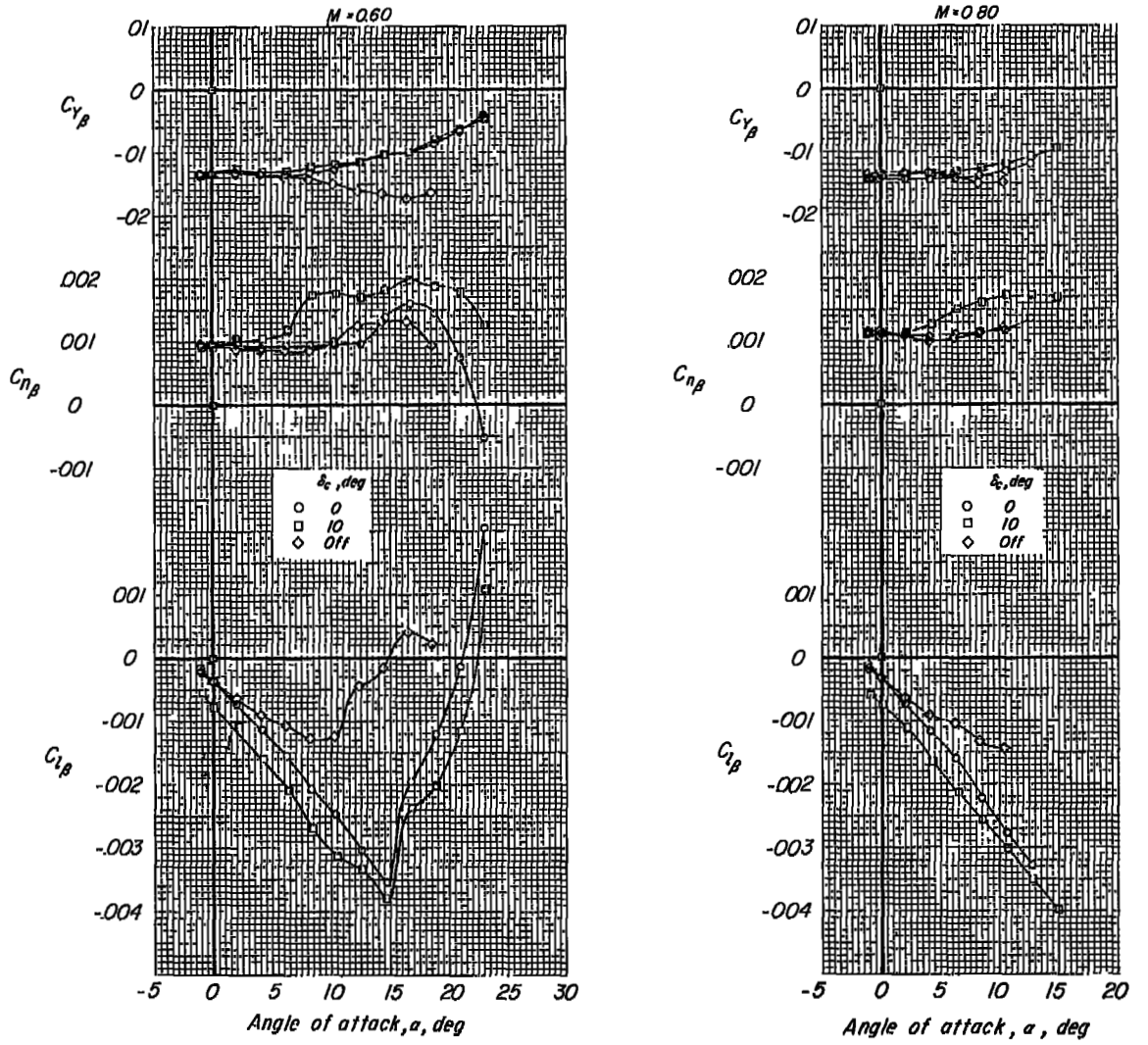

Figure 10.- Effect of the canard surface and canard deflection on the lateral stability derivatives of the delta-wing configuration.

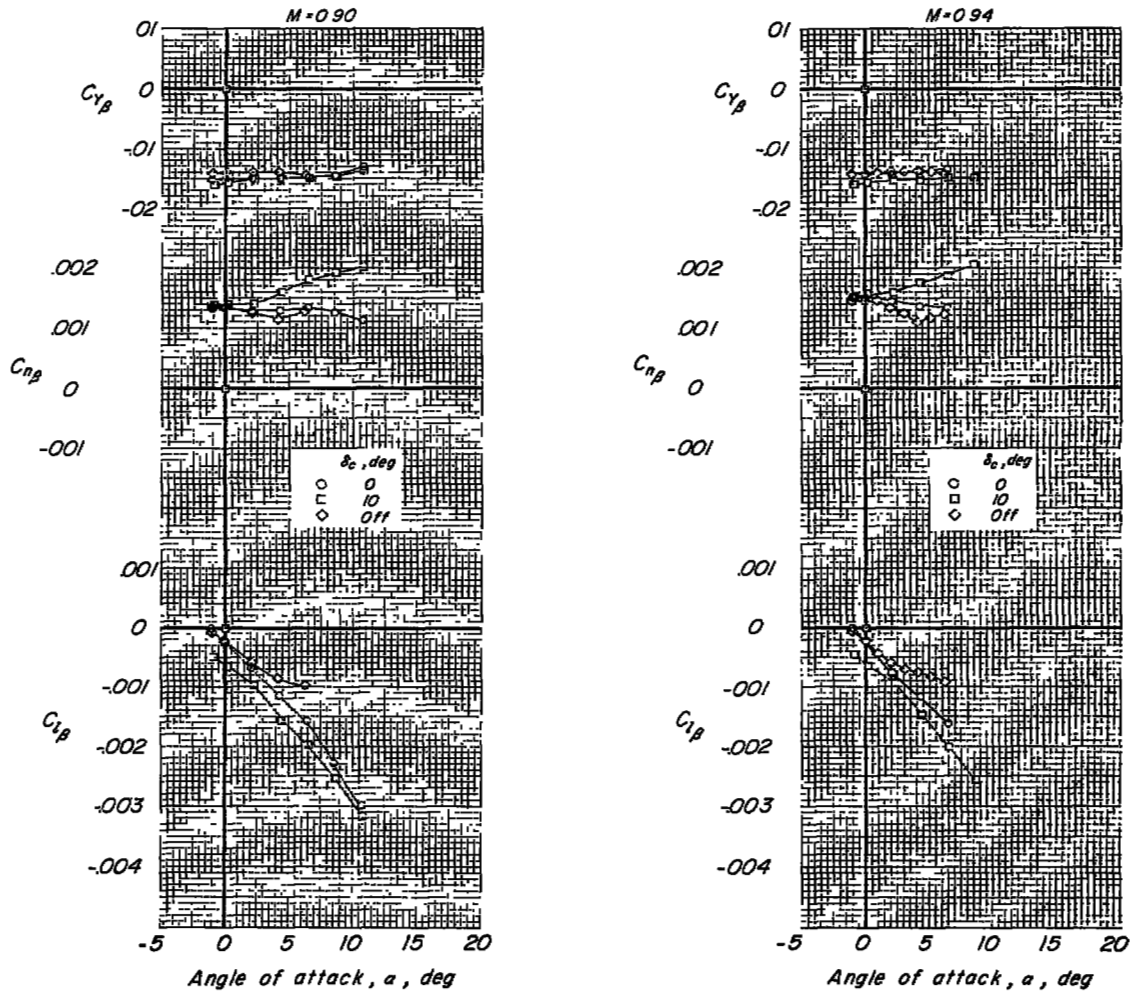

Figure 10.- Concluded.

[redacted]

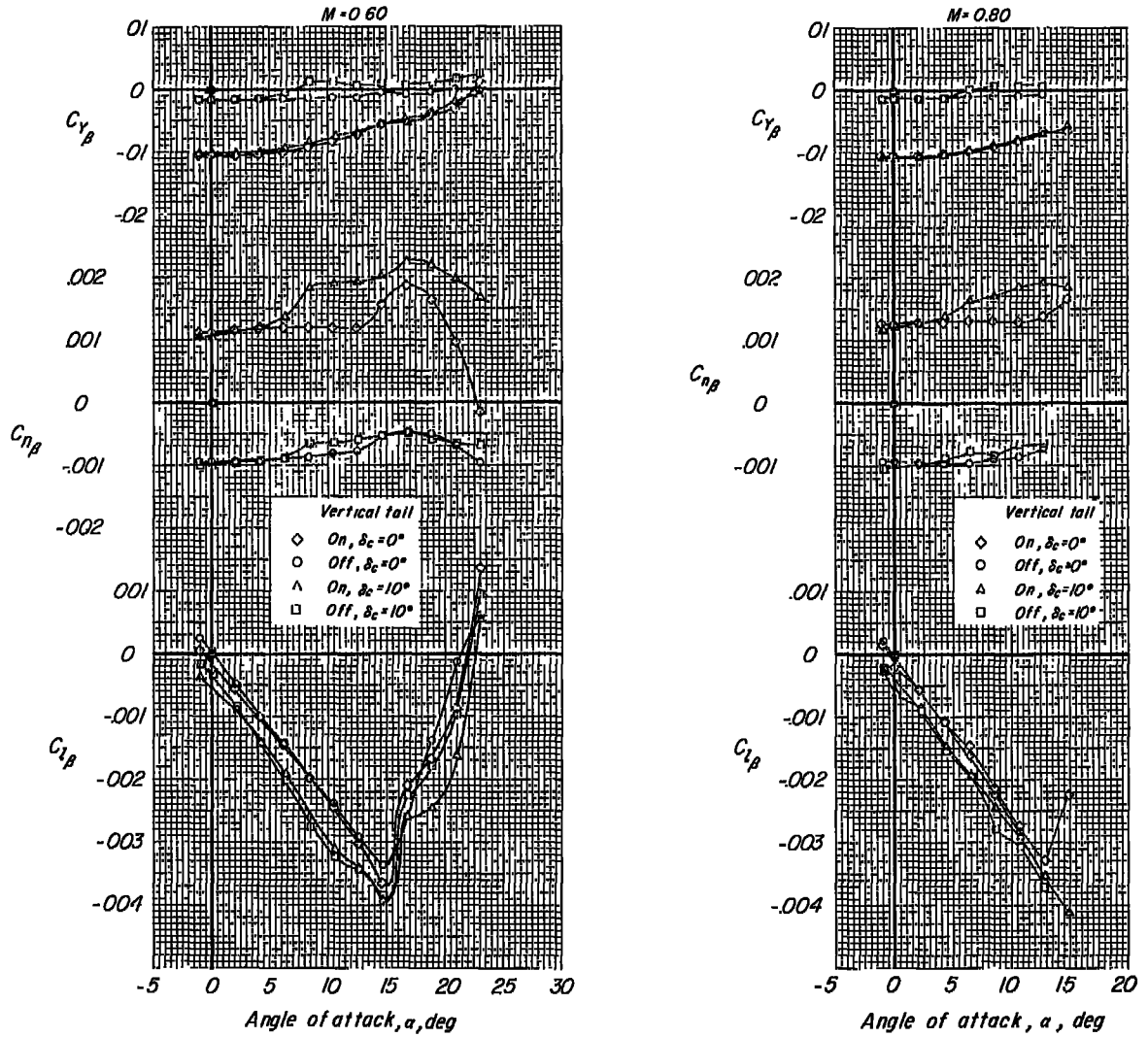

Figure 11.- Effect of the vertical tail on the lateral stability derivatives of the delta-wing configuration with the ventral fins removed.

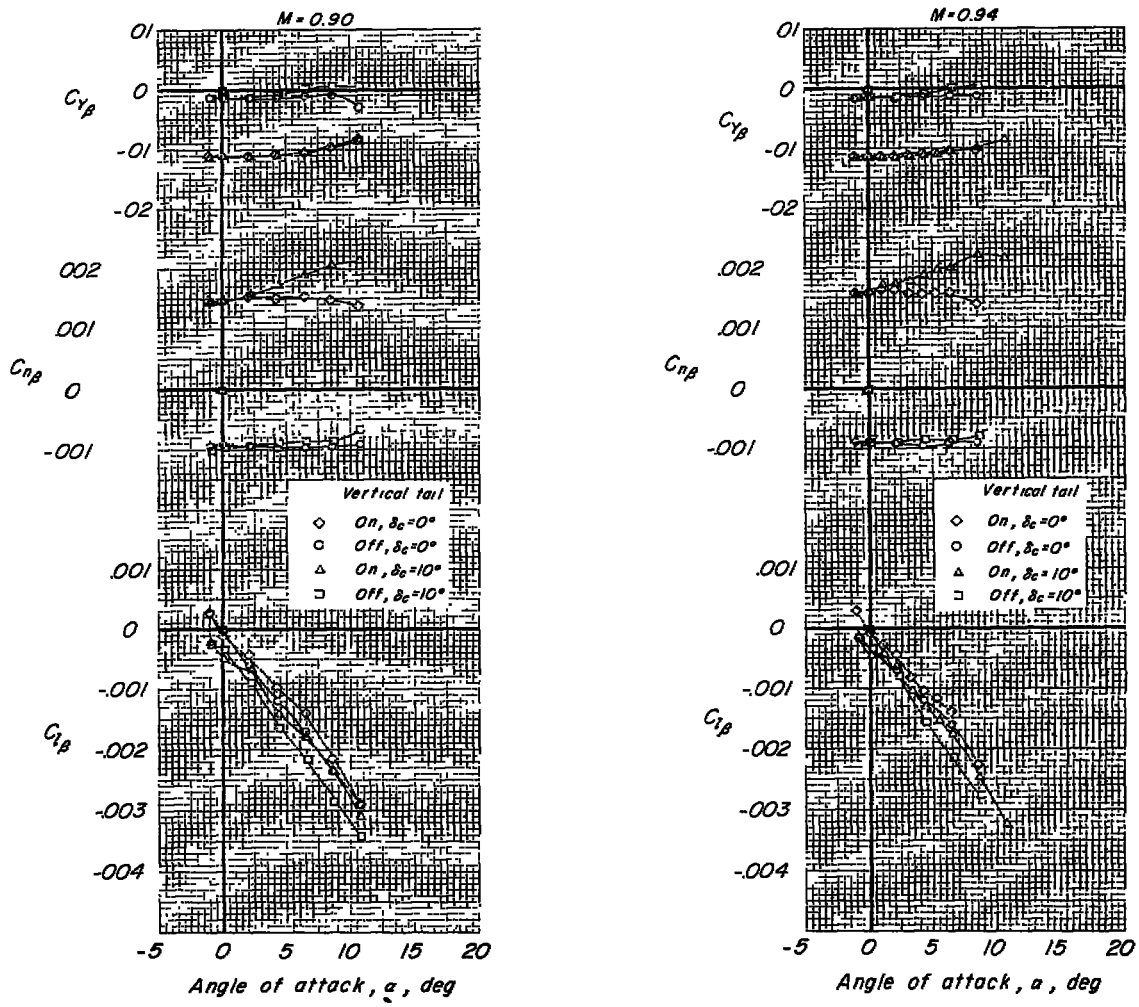

Figure 11.- Concluded.

[redacted]

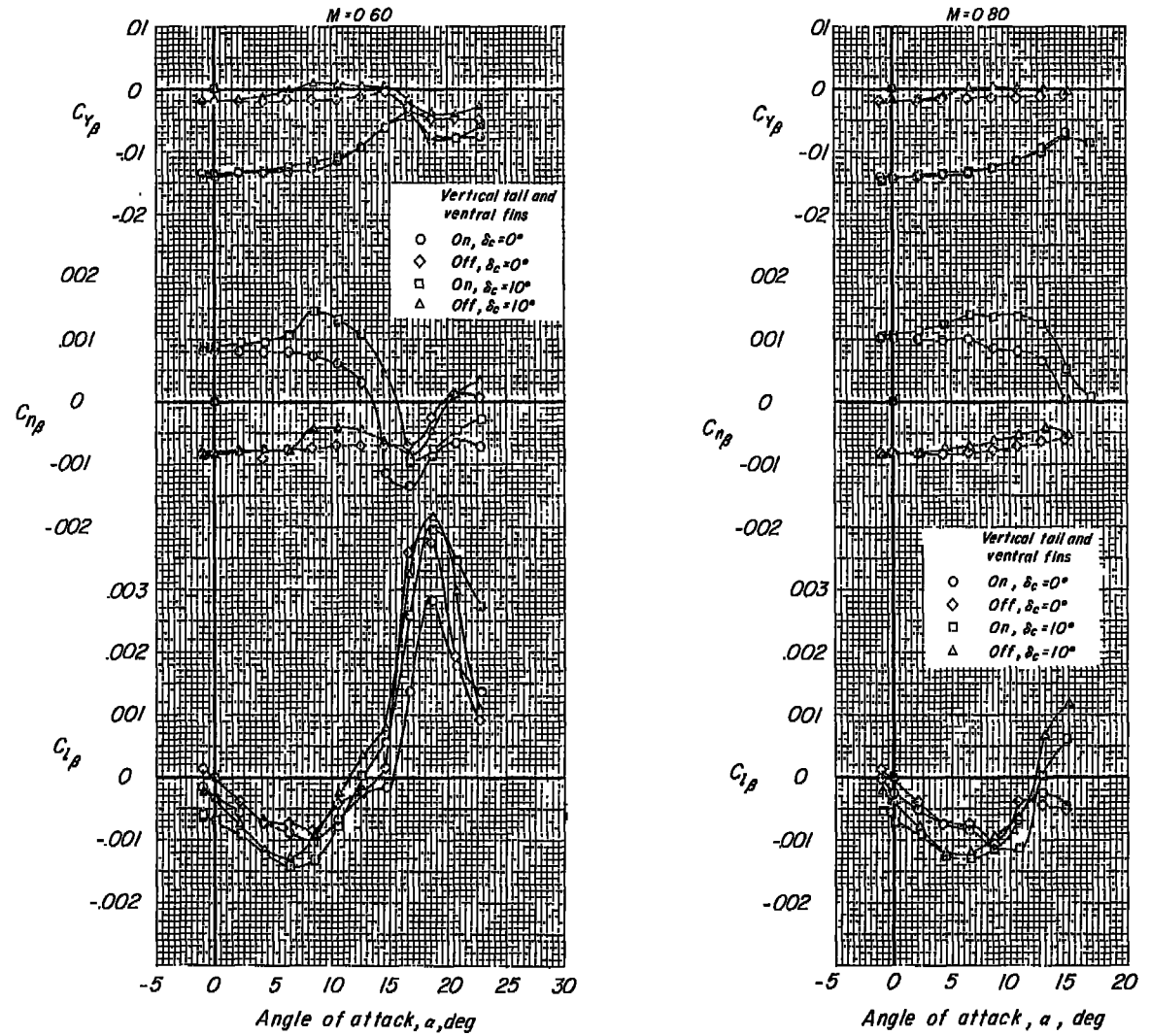

Figure 12.- Effect of both the vertical tail and ventral fins on the lateral stability derivatives of the trapezoid-wing configuration.

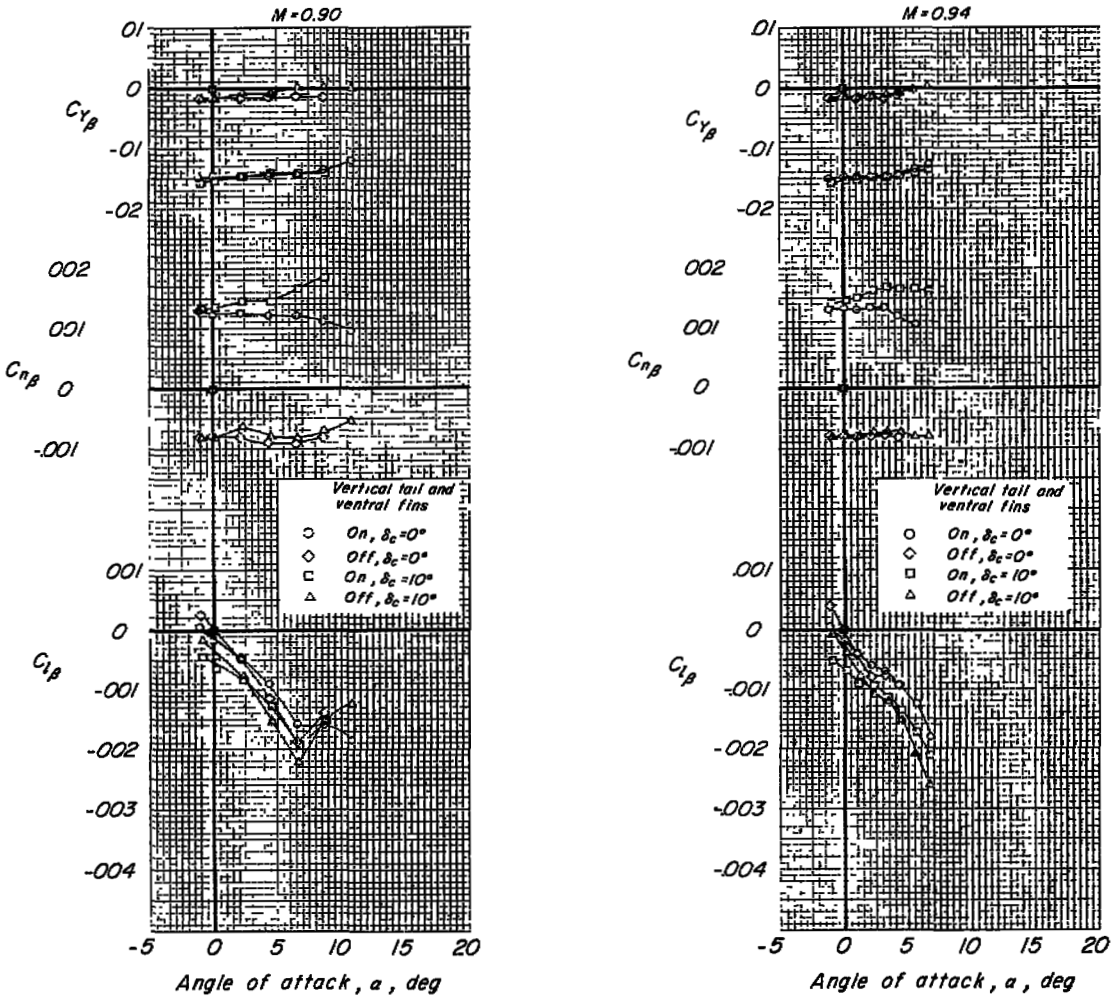

Figure 12.- Concluded.

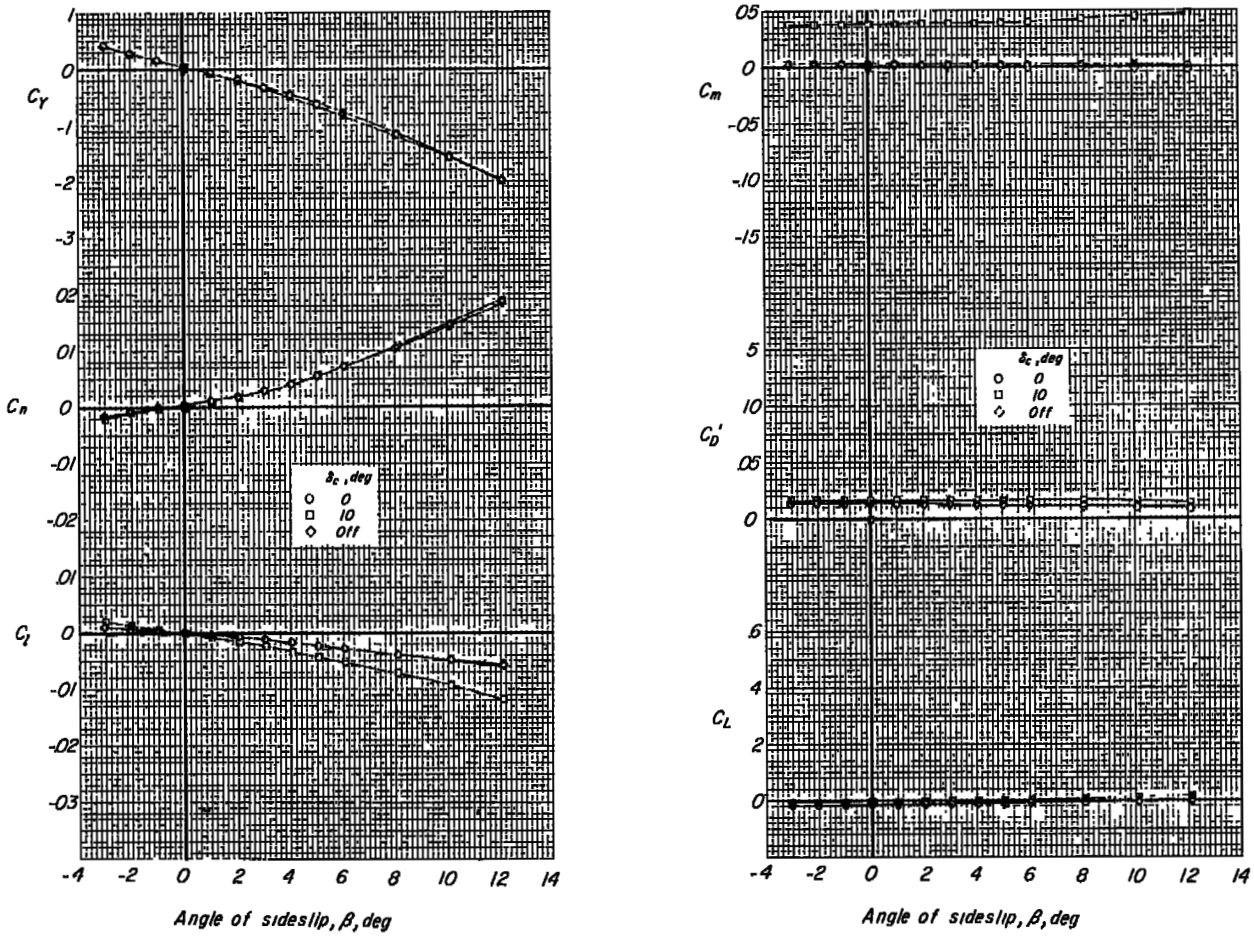

(a) $\alpha \approx 0^\circ$.

Figure 13.- Effect of the canard surface and canard deflection on the aerodynamic characteristics in sideslip of the delta-wing configuration. M = 0.60.

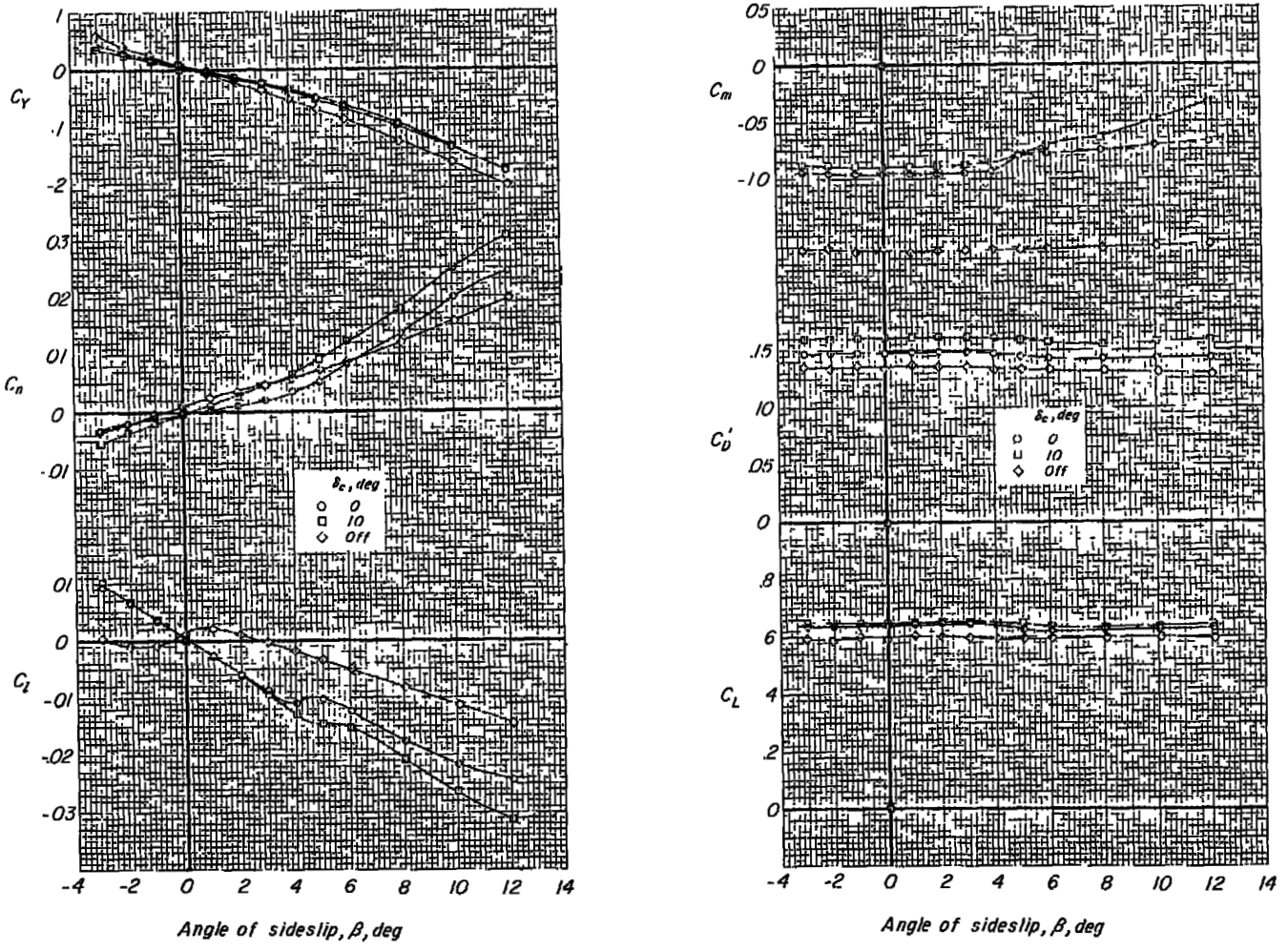

(b) $\alpha \approx 12.5^\circ$.

Figure 13.- Concluded.

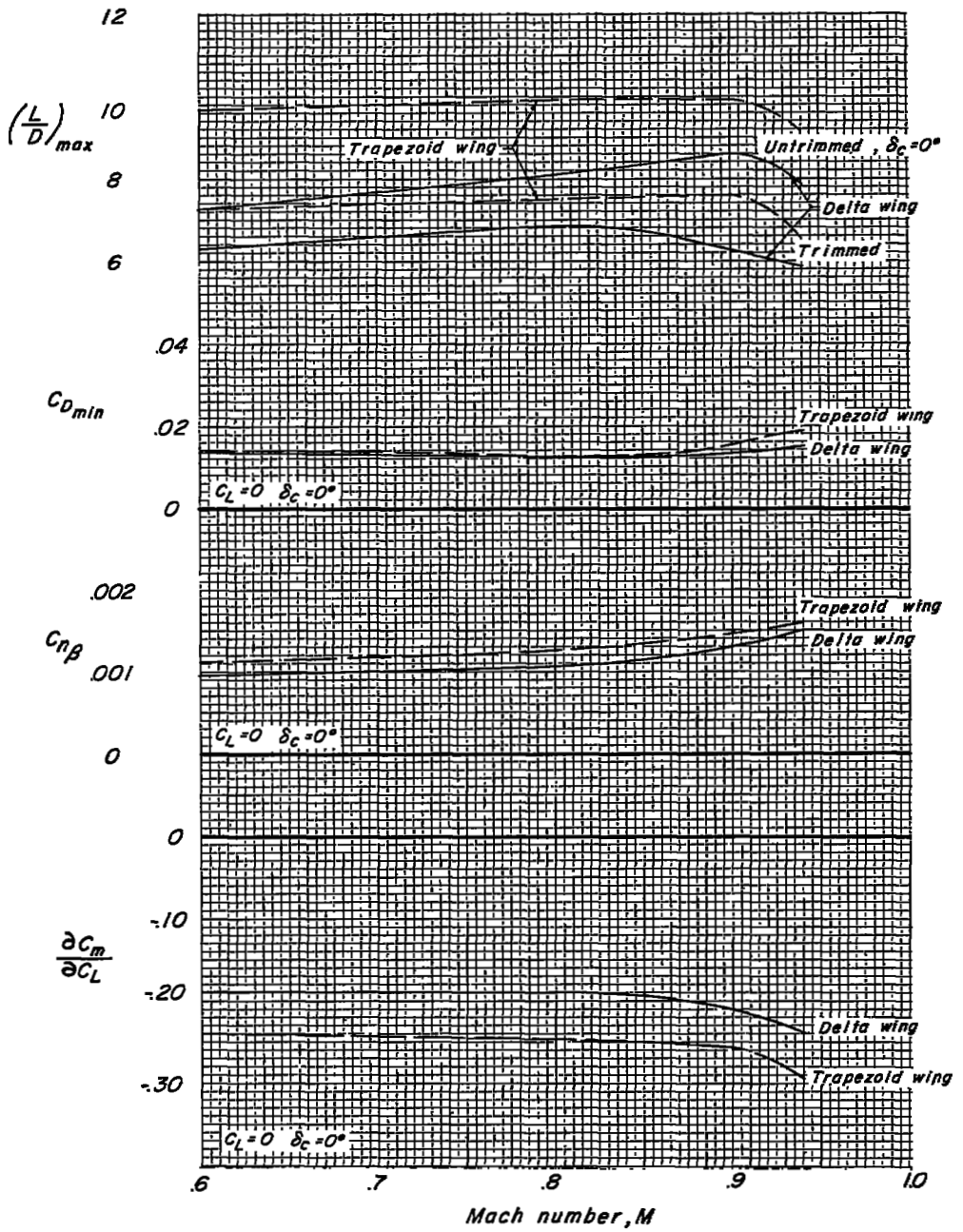

Figure 14.- Variation of static longitudinal and directional stability parameters, minimum drag coefficient, and maximum lift-drag ratio with Mach number.

[redacted]

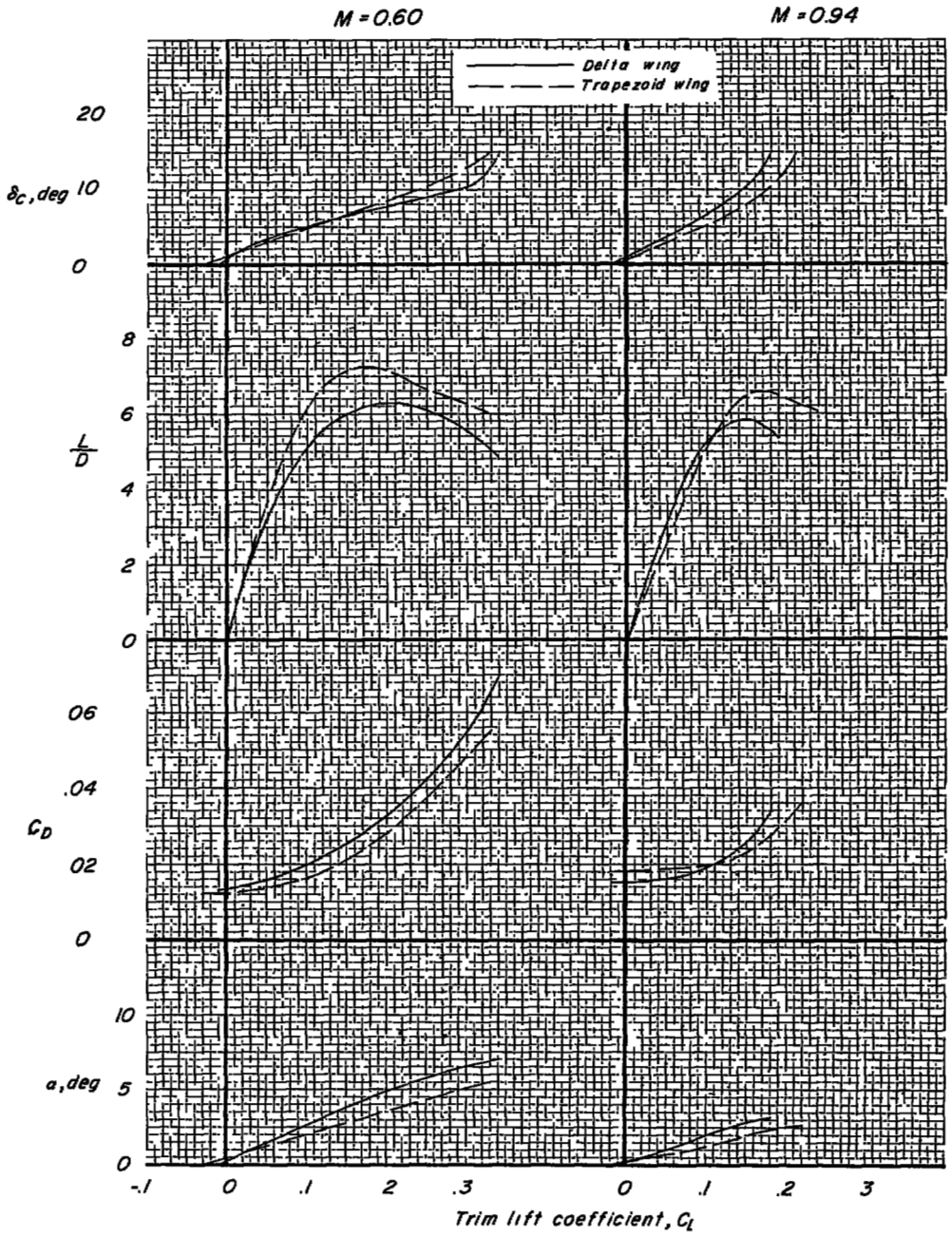

Figure 15.- Variation of longitudinal characteristics for trim conditions of the complete models having the delta wing and the trapezoid wing.

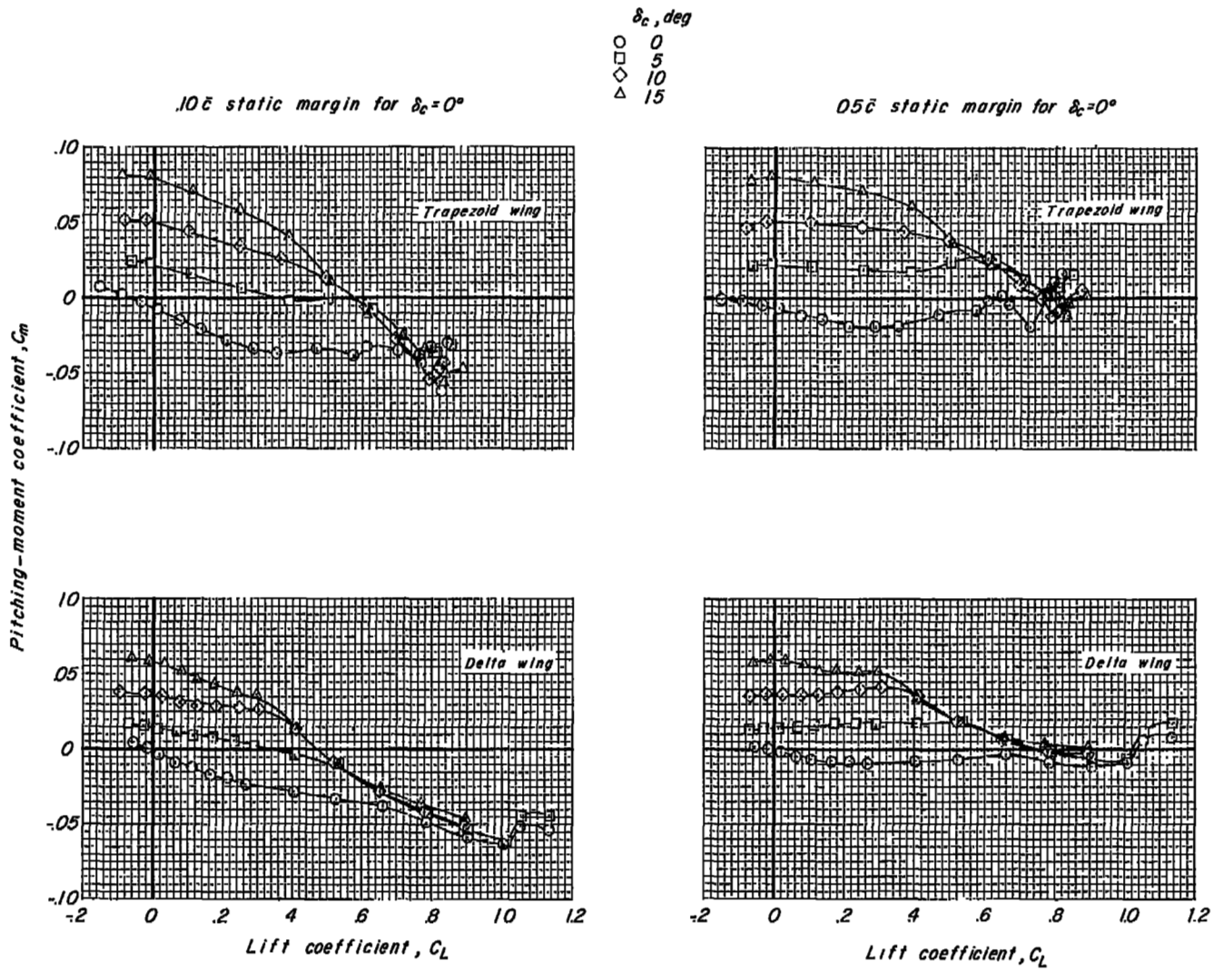

Figure 16.- Pitching-moment characteristics of the models showing control effectiveness of the canard with two values of low-lift static margin. M = 0.60.

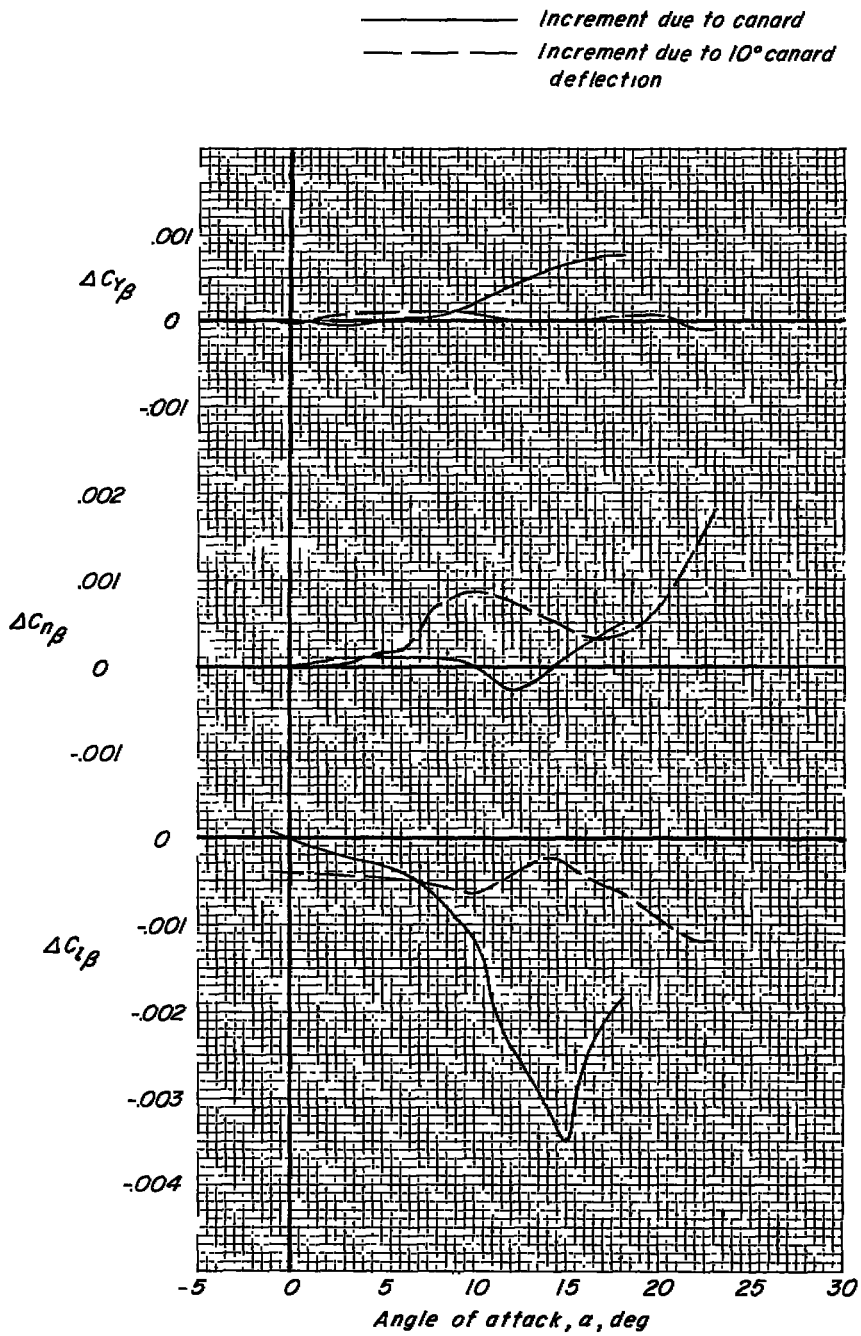

Figure 17.- Increments in lateral stability derivatives due to the canard surface and canard deflection for delta-wing configuration.

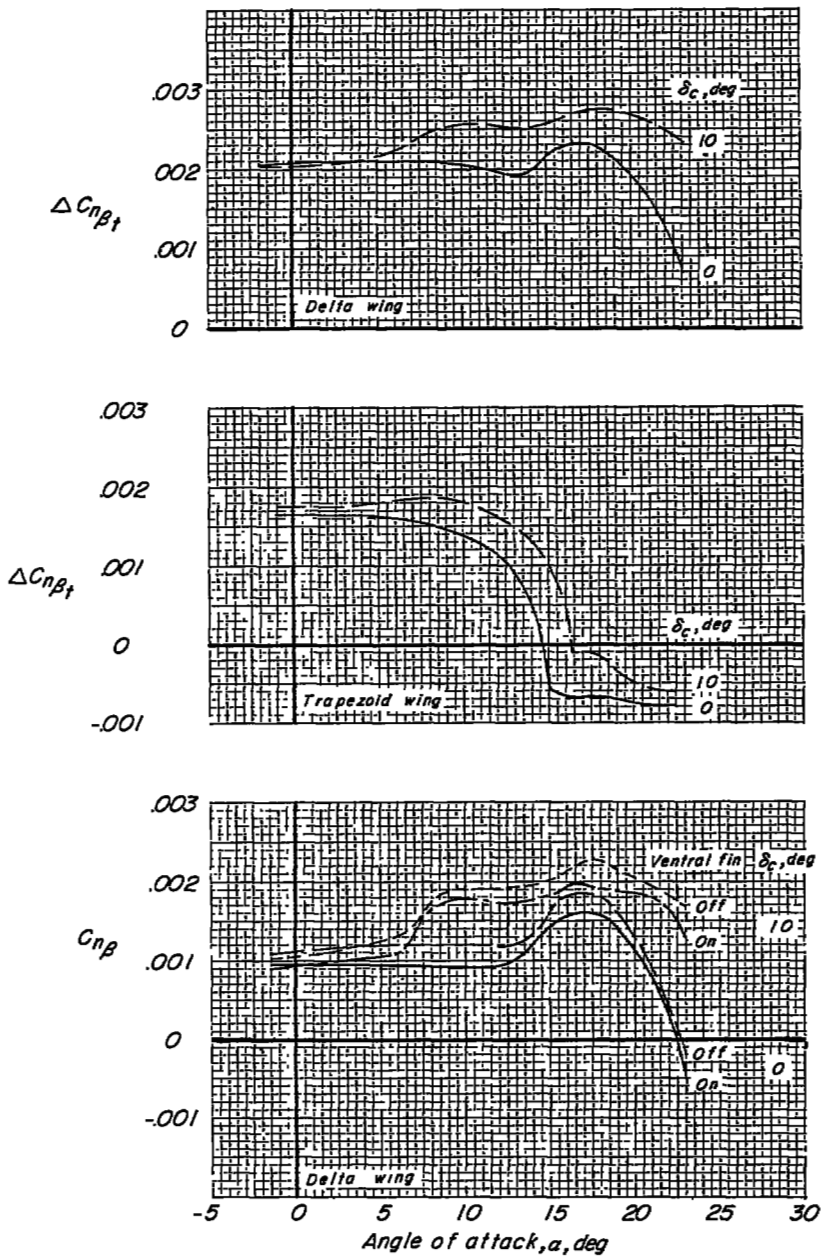

Figure 18.- Effect of canard deflection on the tail contribution to directional stability for the delta-wing and trapezoid-wing models and effect of the ventral fin on the directional stability for the delta-wing configuration. M = 0.60.